

**Mitochondrial respiratory states and rates:
Building blocks of mitochondrial physiology
Part 1.**

http://www.mitoeagle.org/index.php/MitoEAGLE_preprint_2018-02-08

Preprint version 24 (2018-02-16)

MitoEAGLE Network

Corresponding author: Gnaiger E

Contributing co-authors

Acuna-Castroviejo D, Ahn B, Alves MG, Amati F, Aral C, Arandarčikaitė O, Åsander Frostner E, Bailey DM, Bastos Sant'Anna Silva AC, Battino M, Beard DA, Ben-Shachar D, Bishop D, Borutaitė V, Breton S, Brown GC, Brown RA, Buettner GR, Calabria E, Cardoso LHD, Carvalho E, Casado Pinna M, Cervinkova Z, Chang SC, Chen Q, Chicco AJ, Chinopoulos C, Coen PM, Collins JL, Crisóstomo L, Davis MS, Dias T, Distefano G, Doerrier C, Drahota Z, Duchon MR, Ehinger J, Elmer E, Endlicher R, Fell DA, Ferko M, Ferreira JCB, Filipovska A, Fisar Z, Fisher J, Garcia-Roves PM, Garcia-Souza LF, Genova ML, Gonzalo H, Goodpaster BH, Gorr TA, Grefte S, Han J, Harrison DK, Hellgren KT, Hernansanz P, Holland O, Hoppel CL, Houstek J, Hunger M, Iglesias-Gonzalez J, Irving BA, Iyer S, Jackson CB, Jadiya P, Jansen-Dürr P, Jespersen NR, Jha RK, Kaambre T, Kane DA, Kappler L, Karabatsiakakis A, Keijer J, Keppner G, Komlodi T, Kopitar-Jerala N, Krako Jakovljevic N, Kuang J, Kucera O, Labieniec-Watala M, Lai N, Laner V, Larsen TS, Lee HK, Lemieux H, Lerfall J, Lucchinetti E, MacMillan-Crow LA, Makrecka-Kuka M, Meszaros AT, Michalak S, Moiso N, Molina AJA, Montaigne D, Moore AL, Moreira BP, Mracek T, Muntane J, Muntean DM, Murray AJ, Nedergaard J, Nemec M, Newsom S, Nozickova K, O'Gorman D, Oliveira PF, Oliveira PJ, Orynbayeva Z, Pak YK, Palmeira CM, Patel HH, Pecina P, Pereira da Silva Grilo da Silva F, Pesta D, Petit PX, Pichaud N, Pirkmajer S, Porter RK, Pranger F, Prochownik EV, Puurand M, Radenkovic F, Reboredo P, Renner-Sattler K, Robinson MM, Rohlena J, Røslund GV, Rossiter HB, Rybacka-Mossakowska J, Saada A, Salvadego D, Scatena R, Schartner M, Scheibye-Knudsen M, Schilling JM, Schlattner U, Schoenfeld P, Scott GR, Shabalina IG, Sharma P, Shevchuk I, Siewiera K, Singer D, Sobotka O, Sokolova I, Spinazzi M, Stankova P, Stier A, Stocker R, Sumbalova Z, Suravajhala P, Tanaka M, Tandler B, Tepp K, Tomar D, Towheed A, Tretter L, Trivigno C, Tronstad KJ, Trougakos IP, Tyrrell DJ, Urban T, Valentine JM, Velika B, Vendelin M, Vercesi AE, Victor VM, Villena JA, Wagner BA, Ward ML, Watala C, Wei YH, Wieckowski MR, Wohlwend M, Wolff J, Wuest RCI, Zaugg K, Zaugg M, Zorzano A

Supporting co-authors:

Bakker BM, Bernardi P, Boetker HE, Borsheim E, Bouitbir J, Calbet JA, Calzia E, Chaurasia B, Clementi E, Coker RH, Collin A, Das AM, De Palma C, Dubouchaud H, Durham WJ, Dyrstad SE, Engin AB, Fornaro M, Gan Z, Garlid KD, Garten A, Gourlay CW, Granata C, Haas CB, Haavik J, Haendeler J, Hand SC, Hepple RT, Hickey AJ, Hoel F, Jang DH, Kainulainen H, Khamoui AV, Klingenspor M, Koopman WJH, Kowaltowski AJ, Krajcova A, Lane N, Lenaz G, Malik A, Markova M, Mazat JP, Menze MA, Methner A, Neuzil J, Oliveira MT, Pallotta ML, Parajuli N, Pettersen IKN, Porter C, Pulinilkunnil T, Ropelle ER, Salin K, Sandi C, Sazanov LA, Silber AM, Skolik R, Smenes BT, Soares FAA, Sonkar VK, Swerdlow RH, Szabo I, Trifunovic A, Thyfault JP, Vieyra A, Votion DM, Williams C, Zischka H

Updates and discussion:

http://www.mitoeagle.org/index.php/MitoEAGLE_preprint_2018-02-08

Correspondence: Gnaiger E

Chair COST Action CA15203 MitoEAGLE – <http://www.mitoeagle.org>

*Department of Visceral, Transplant and Thoracic Surgery, D. Swarovski Research
Laboratory, Medical University of Innsbruck, Innrain 66/4, A-6020 Innsbruck, Austria*

Email: erich.gnaiger@i-med.ac.at

Tel: +43 512 566796, Fax: +43 512 566796 20

Contents**Abstract****Executive summary****1. Introduction** – Box 1: In brief: Mitochondria and Bioblasts**2. Oxidative phosphorylation and coupling states in mitochondrial preparations**

Mitochondrial preparations

2.1. Respiratory control and coupling

The steady-state

Specification of biochemical dose

Phosphorylation, P_{\gg} , and P_{\gg}/O_2 ratio

Control and regulation

Respiratory control and response

Respiratory coupling control and ET-pathway control

Coupling

Uncoupling

2.2. Coupling states and respiratory rates

Respiratory capacities in coupling control states

LEAK, OXPHOS, ET, ROX

2.3. Classical terminology for isolated mitochondria

States 1–5

3. Normalization: fluxes and flows*3.1. Normalization: system or sample*

Flow per system, I

Extensive quantities

Size-specific quantities – Box 2: Metabolic fluxes and flows: vectorial and scalar

3.2. Normalization for system-size: flux per chamber volume

System-specific flux, J

3.3. Normalization: per sample

Sample concentration, C_{mX}

Mass-specific flux, J_{mX,O_2}

Number concentration, C_{NX}

Flow per object, I_{X,O_2}

3.4. Normalization for mitochondrial content

Mitochondrial concentration, C_{mtE} , and mitochondrial markers

Mitochondria-specific flux, J_{mtE,O_2}

*3.5. Evaluation of mitochondrial markers**3.6. Conversion: units***4. Conclusions** – Box 3: Mitochondrial and cell respiration**5. References**

102 **Abstract** As the knowledge base and importance of mitochondrial physiology to human health
103 expand, the necessity for harmonizing nomenclature concerning mitochondrial respiratory
104 states and rates has become increasingly apparent. Clarity of concept and consistency of
105 nomenclature are key trademarks of a research field. These trademarks facilitate effective
106 transdisciplinary communication, education, and ultimately further discovery. Peter Mitchell's
107 chemiosmotic theory establishes the mechanism of energy transformation and coupling in
108 oxidative phosphorylation. The unifying concept of the protonmotive force provides the
109 framework for developing a consistent theory and nomenclature for mitochondrial physiology
110 and bioenergetics. Herein, we follow IUPAC guidelines on general terms of physical chemistry,
111 extended by considerations on open systems and irreversible thermodynamics. We align the
112 nomenclature and symbols of classical bioenergetics with a concept-driven constructive
113 terminology to express the meaning of each quantity clearly and consistently. In this position
114 statement, in the frame of COST Action MitoEAGLE, we endeavour to provide a balanced
115 view on mitochondrial respiratory control and a critical discussion on reporting data of
116 mitochondrial respiration in terms of metabolic flows and fluxes. Uniform standards for
117 evaluation of respiratory states and rates will ultimately support the development of databases
118 of mitochondrial respiratory function in species, tissues, and cells.

119

120 *Keywords:* Mitochondrial respiratory control, coupling control, mitochondrial
121 preparations, protonmotive force, oxidative phosphorylation, OXPHOS, efficiency, electron
122 transfer, ET; proton leak, LEAK, residual oxygen consumption, ROX, State 2, State 3, State 4,
123 normalization, flow, flux

124

125

126

127

127 **Executive summary**

128

129

130

131

132

133

134

135

136

137

138

139

140

141

142

143

144

145

146

147

148

149

150

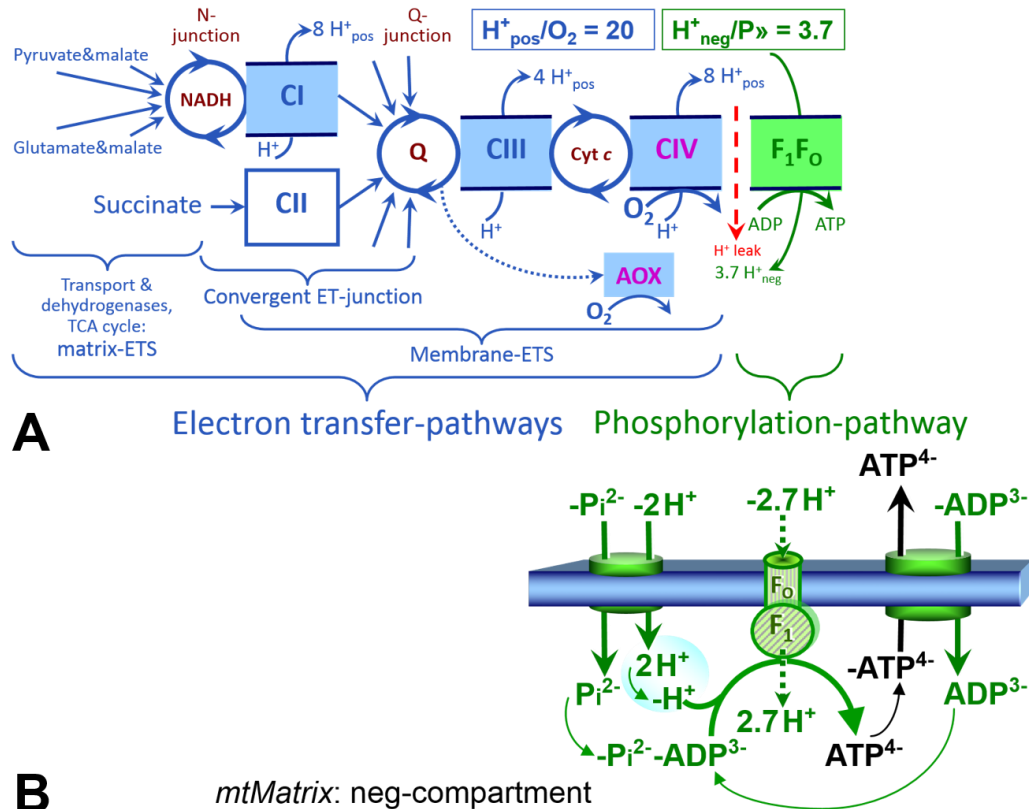
151

152

1. In view of broad implications on health care, mitochondrial researchers face an increasing responsibility to disseminate their fundamental knowledge and novel discoveries to a wide range of stakeholders and scientists beyond the group of specialists. This requires implementation of a commonly accepted terminology within the discipline and standardization in the translational context. Authors, reviewers, journal editors, and lecturers are challenged to collaborate with the aim to harmonize the nomenclature in the growing field of mitochondrial physiology and bioenergetics.
2. Aerobic energy metabolism in mammalian mitochondria depends on the coupling of ADP → ATP phosphorylation to oxygen consumption in catabolic reactions. In this process of oxidative phosphorylation, coupling is mediated by translocation of protons through respiratory proton pumps operating across the inner mitochondrial membrane and generating or utilizing the protonmotive force measured between the mitochondrial matrix and intermembrane compartment. Compartmental—or vectorial—coupling thus distinguishes respiration from fermentation as the counterpart of cellular core energy metabolism.
3. To exclude fermentation and other cytosolic interactions from exerting an effect on mitochondrial metabolism, the barrier function of the plasma membrane must be disrupted. Selective removal or permeabilization of the plasma membrane yields mitochondrial preparations—including isolated mitochondria, tissue and cellular preparations—with structural and functional integrity. Then extra-mitochondrial concentrations of fuel substrates transported into the mitochondrial matrix, ADP, ATP, inorganic phosphate, and cations including H⁺ can be controlled to determine mitochondrial function under a set of conditions defined as coupling

153
154
155
156
157

control states. A concept-driven terminology of bioenergetics incorporates in its terms and symbols explicitly information on the nature of respiratory states, that makes the technical terms readily recognized and easy to understand.



158
159
160
161
162
163
164
165
166
167
168
169
170
171
172
173
174
175
176
177
178
179
180

Fig. 1. The oxidative phosphorylation (OXPHOS) system. (A) The mitochondrial electron transfer system (ETS) is fuelled by diffusion and transport of substrates across the mtOM and mtIM. It consists of the matrix-ETS and membrane-ETS. ET-pathways are coupled to the phosphorylation-pathway. ET-pathways converge at the N-junction and Q-junction. Additional arrows indicate electron entry into the Q-junction through electron transferring flavoprotein, glycerophosphate dehydrogenase, dihydro-orotate dehydrogenase, choline dehydrogenase, and sulfide-ubiquinone oxidoreductase. The dotted arrow indicates the branched pathway of oxygen consumption by alternative quinol oxidase (AOX). The H^+_{pos}/O_2 ratio is the outward proton flux from the matrix space to the positively (pos) charged compartment, divided by catabolic O_2 flux in the NADH-pathway. The H^+_{neg}/P ratio is the inward proton flux from the inter-membrane space to the negatively (neg) charged matrix space, divided by the flux of phosphorylation of ADP to ATP (Eq. 1). These are not fixed stoichiometries due to ion leaks and proton slip. (B) Phosphorylation-pathway catalyzed by the proton pump F₁F₀-ATPase (F-ATPase), adenine nucleotide translocase, and inorganic phosphate transporter. The H^+_{neg}/P stoichiometry is the sum of the coupling stoichiometry in the F-ATPase reaction ($-2.7 H^+_{\text{pos}}$ from the positive intermembrane space, $2.7 H^+_{\text{neg}}$ to the matrix, *i.e.*, the negative compartment) and the proton balance in the translocation of ADP²⁻, ATP³⁻ and Pi²⁻. Modified from (A) Lemieux *et al.* (2017) and (B) Gnaiger (2014).

4. Mitochondrial coupling states are defined according to the control of respiratory oxygen consumption by the protonmotive force. Capacities of oxidative phosphorylation

181 and electron transfer capacities are measured at kinetically saturating
 182 concentrations of fuel substrates, ADP and inorganic phosphate, or at optimal
 183 uncoupler concentrations, respectively. Respiratory capacities are a measure of the
 184 upper bound of the rates of respiration, providing reference values for the diagnosis
 185 of health and disease, and for evaluation of the effects of Evolutionary background,
 186 Age, Gender and sex, Lifestyle and Environment (EAGLE).

- 187 5. Some degree of uncoupling is a characteristic of energy-transformations across
 188 membranes. Uncoupling is caused by a variety of physiological, pathological,
 189 toxicological, pharmacological and environmental conditions that exert an
 190 influence not only on the proton leak and cation cycling, but also on proton slip
 191 within the proton pumps and the structural integrity of the mitochondria. A more
 192 loosely coupled state is induced by stimulation of mitochondrial superoxide anion
 193 radical formation and the bypass of proton pumps. In addition, uncoupling by
 194 application of protonophores represents an experimental intervention for the
 195 transition from a well-coupled to the noncoupled state of mitochondrial respiration.
- 196 6. Respiratory oxygen consumption rates have to be carefully normalized to provide valid
 197 information and enable meta-analytic studies beyond the specific question of a
 198 particular experiment. Therefore, all raw data should be published in a supplemental
 199 table or open access data repository. Normalization of rates for the volume of the
 200 experimental chamber (the measuring system) is distinguished from normalization
 201 for (1) the volume or mass of the experimental sample, (2) the number of objects
 202 (cells, organisms), and (3) the concentration of mitochondrial markers in the
 203 chamber.
- 204 7. The consistent use of terms and symbols discussed in this MitoEAGLE position
 205 statement will facilitate transdisciplinary communication and support further
 206 developments of a database on bioenergetics and mitochondrial physiology. The
 207 present recommendations are focused on studies with mitochondrial preparations.
 208 These will be extended in a series of reports on pathway control of mitochondrial
 209 respiration, respiratory states in intact cells, and harmonization of experimental
 210 procedures.

211
 212
 213
 214

215 **Box 1: In brief – Mitochondria and Bioblasts**

216
 217 **Mitochondria** are the oxygen-consuming electrochemical generators evolved from
 218 endosymbiotic bacteria (Margulis 1970; Lane 2005). They were described by Richard Altmann
 219 (1894) as ‘bioblasts’, which include not only the mitochondria as presently defined, but also
 220 symbiotic and free-living bacteria. The word ‘mitochondria’ (Greek mitos: thread; chondros:
 221 granule) was introduced by Carl Benda (1898).

222 Mitochondrial dysfunction is associated with a wide variety of genetic and degenerative
 223 diseases. Robust mitochondrial function is supported by physical exercise and caloric balance,
 224 and is central for sustained metabolic health throughout life. Therefore, a more consistent
 225 presentation of mitochondrial physiology will improve our understanding of the etiology of
 226 disease, the diagnostic repertoire of mitochondrial medicine, with a focus on protective
 227 medicine, lifestyle and healthy aging.

228 We now recognize mitochondria as dynamic organelles with a double membrane that are
 229 contained within eukaryotic cells. The mitochondrial inner membrane (mtIM) shows dynamic
 230 tubular to disk-shaped cristae that separate the mitochondrial matrix, *i.e.*, the negatively charged
 231 internal mitochondrial compartment, and the intermembrane space; the latter being positively

232 charged and enclosed by the mitochondrial outer membrane (mtOM). The mtIM contains the
 233 non-bilayer phospholipid cardiolipin, which is not present in any other eukaryotic cellular
 234 membrane. Cardiolipin promotes the formation of respiratory supercomplexes, which are
 235 supramolecular assemblies based upon specific, though dynamic, interactions between
 236 individual respiratory complexes (Greggio *et al.* 2017; Lenaz *et al.* 2017). Membrane fluidity
 237 **exters** influence on functional properties of proteins incorporated in the membranes
 238 (Waczulikova *et al.* 2007).

239 Mitochondria are the structural and functional elements of cell respiration. Cell
 240 respiration is the consumption of oxygen by electron transfer coupled to electrochemical proton
 241 translocation across the mtIM. In the process of oxidative phosphorylation (OXPHOS), the
 242 reduction of O₂ is electrochemically coupled to the transformation of energy in the form of
 243 adenosine triphosphate (ATP; Mitchell 1961, 2011). Mitochondria are the powerhouses of the
 244 cell which contain the machinery of the OXPHOS-pathways, including transmembrane
 245 respiratory complexes—proton pumps with FMN, Fe-S and cytochrome *b*, *c*, *aa₃* redox
 246 systems); alternative dehydrogenases and oxidases; the coenzyme ubiquinone (Q); F-ATPase
 247 or ATP synthase; the enzymes of the tricarboxylic acid cycle and fatty acid oxidation;
 248 transporters of ions, metabolites and co-factors; and mitochondrial kinases related to energy
 249 transfer pathways. The mitochondrial proteome comprises over 1,200 proteins (Calvo *et al.*
 250 2015; 2017), mostly encoded by nuclear DNA (nDNA), with a variety of functions, many of
 251 which are relatively well known (*e.g.*, apoptosis-regulating proteins), while others are still under
 252 investigation, or need to be identified (*e.g.*, alanine transporter).

253 There is a constant crosstalk between mitochondria and the other cellular components.
 254 The crosstalk between mitochondria and endoplasmic reticulum is involved in the regulation of
 255 calcium homeostasis, cell division, autophagy, differentiation, anti-viral signaling (Murley and
 256 Nunnari 2016). Cellular mitostasis is maintained through regulation at both the transcriptional
 257 and post-translational level, through cell signalling including proteostatic (*e.g.*, the ubiquitin-
 258 proteasome and autophagy-lysosome pathways), and genome stability modules throughout the
 259 cell cycle or even cell death, contributing to homeostatic regulation in response to varying
 260 energy demands and stress (Quiros *et al.* 2016). In addition to mitochondrial movement along
 261 the microtubules, mitochondrial morphology can change in response to energy requirements of
 262 the cell via processes known as fusion and fission, through which mitochondria communicate
 263 within a network, and in response to intracellular stress factors causing swelling and ultimately
 264 permeability transition.

265 Mitochondria typically maintain several copies of their own genome known as
 266 mitochondrial DNA (mtDNA; hundred to thousands per cell; Cummins 1998), which is
 267 maternally inherited. One exception to strictly maternal inheritance in animals is found in
 268 bivalves (Breton *et al.* 2007; White *et al.* 2008). mtDNA is 16.5 kB in length, contains 13
 269 protein-coding genes for subunits of the transmembrane respiratory Complexes CI, CIII, CIV
 270 and F-ATPase, and also encodes 22 tRNAs and the mitochondrial 16S and 12S rRNA.
 271 Additional gene content is encoded in the mitochondrial genome, *e.g.*, microRNAs, piRNA,
 272 smithRNAs, repeat associated RNA, and even additional proteins (Duarte *et al.* 2014; Lee *et al.*
 273 2015; Cobb *et al.* 2016). The mitochondrial genome is regulated and supplemented by
 274 nuclear-encoded **mitochondrial** targeted proteins.

275 Abbreviation: mt, as generally used in mtDNA. Mitochondrion is singular and
 276 mitochondria is plural.

277 ‘For the physiologist, mitochondria afforded the first opportunity for an experimental
 278 approach to structure-function relationships, in particular those involved in active transport,
 279 vectorial metabolism, and metabolic control mechanisms on a subcellular level’ (Ernster and
 280 Schatz 1981).

281
 282

283
284
285

1. Introduction

286 Mitochondria are the powerhouses of the cell with numerous physiological, molecular,
287 and genetic functions (**Box 1**). Every study of mitochondrial health and disease is faced with
288 Evolution, Age, Gender and sex, Lifestyle, and Environment (EAGLE) as essential background
289 conditions intrinsic to the individual patient or subject, cohort, species, tissue and to some extent
290 even cell line. As a large and coordinated group of laboratories and researchers, the mission of
291 the global MitoEAGLE Network is to generate the necessary scale, type, and quality of
292 consistent data sets and conditions to address this intrinsic complexity. Harmonization of
293 experimental protocols and implementation of a quality control and data management system
294 are required to interrelate results gathered across a spectrum of studies and to generate a
295 rigorously monitored database focused on mitochondrial respiratory function. In this way,
296 researchers within the same and across different disciplines will be positioned to compare
297 findings across traditions and generations to an agreed upon set of clearly defined and accepted
298 international standards.

299 Reliability and comparability of quantitative results depend on the accuracy of
300 measurements under strictly-defined conditions. A conceptual framework is required to warrant
301 meaningful interpretation and comparability of experimental outcomes carried out by research
302 groups at different institutes. With an emphasis on quality of research, collected data can be
303 useful far beyond the specific question of a particular experiment. Enabling meta-analytic
304 studies is the most economic way of providing robust answers to biological questions (Cooper
305 *et al.* 2009). Vague or ambiguous jargon can lead to confusion and may relegate valuable
306 signals to wasteful noise. For this reason, measured values must be expressed in standard units
307 for each parameter used to define mitochondrial respiratory function. Harmonization of
308 nomenclature and definition of technical terms are essential to improve the awareness of the
309 intricate meaning of current and past scientific vocabulary, for documentation and integration
310 into databases in general, and quantitative modelling in particular (Beard 2005). The focus on
311 coupling states and fluxes through metabolic pathways of aerobic energy transformation in
312 mitochondrial preparations is a first step in the attempt to generate a conceptually-oriented
313 nomenclature in bioenergetics and mitochondrial physiology. Coupling states of intact cells,
314 the protonmotive force, and respiratory control by fuel substrates and specific inhibitors of
315 respiratory enzymes will be reviewed in subsequent communications.

316
317

2. Oxidative phosphorylation and coupling states in mitochondrial preparations

319 *‘Every professional group develops its own technical jargon for talking about matters of*
320 *critical concern ... People who know a word can share that idea with other members of*
321 *their group, and a shared vocabulary is part of the glue that holds people together and*
322 *allows them to create a shared culture’ (Miller 1991).*

323

324 **Mitochondrial preparations** are defined as either isolated mitochondria, or tissue and
325 cellular preparations in which the barrier function of the plasma membrane is disrupted. The
326 plasma membrane separates the cytosol, nucleus, and organelles (the intracellular
327 compartment) from the environment of the cell. The plasma membrane consists of a lipid
328 bilayer, embedded proteins, and attached organic molecules that collectively control the
329 selective permeability of ions, organic molecules, and particles across the cell boundary. The
330 intact plasma membrane prevents the passage of many water-soluble mitochondrial substrates
331 and inorganic ions—such as succinate, adenosine diphosphate (ADP) and inorganic phosphate
332 (P_i), that must be controlled at kinetically-saturating concentrations for the analysis of

333 respiratory capacities; this limits the scope of investigations into mitochondrial respiratory
334 function in intact cells.

335 The cholesterol content of the plasma membrane is high compared to mitochondrial
336 membranes. Therefore, mild detergents—such as digitonin and saponin—can be applied to
337 selectively permeabilize the plasma membrane by interaction with cholesterol and allow free
338 exchange of organic molecules and inorganic ions between the cytosol and the immediate cell
339 environment, while maintaining the integrity and localization of organelles, cytoskeleton, and
340 the nucleus. Application of optimum concentrations of permeabilization agents (mild detergents
341 or toxins) leads to the complete loss of cell viability, tested by nuclear staining and washout of
342 cytosolic marker enzymes—such as lactate dehydrogenase, while mitochondrial function
343 remains intact. The respiration rate of isolated mitochondria remains unaltered after the addition
344 of low concentrations of digitonin or saponin. In addition to mechanical permeabilization during
345 homogenization of tissue, permeabilization agents may be applied to ensure permeabilization
346 of all cells. Suspensions of cells permeabilized in the respiration chamber and crude tissue
347 homogenates contain all components of the cell at highly diluted concentrations. All
348 mitochondria are retained in chemically-permeabilized mitochondrial preparations and crude
349 tissue homogenates. In the preparation of isolated mitochondria, the cells or tissues are
350 homogenized, and the mitochondria are separated from other cell fractions and purified by
351 differential centrifugation, entailing the loss of a fraction of mitochondria. Typical
352 mitochondrial recovery ranges from 30% to 80%. Maximization of the purity of isolated
353 mitochondria may compromise not only the mitochondrial yield but also the structural and
354 functional integrity. Therefore, protocols to isolate mitochondria need to be optimized
355 according to each study. The term mitochondrial preparation does not include further
356 fractionation of mitochondrial components, neither submitochondrial particles.

357

358 *2.1. Respiratory control and coupling*

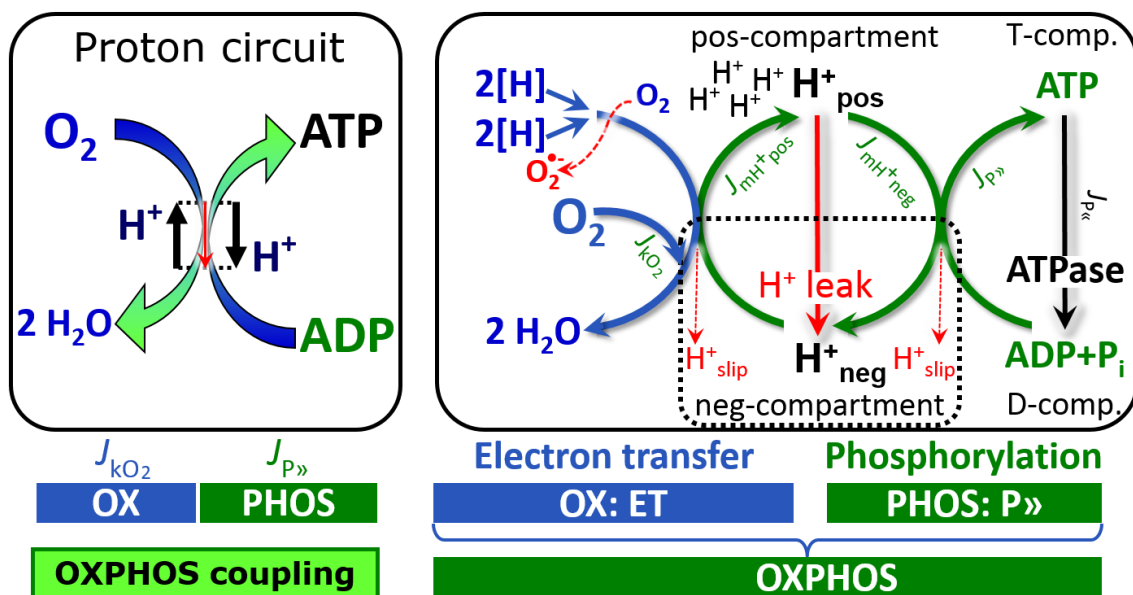
359

360 Respiratory coupling control states are established in the study of mitochondrial
361 preparations to obtain reference values for various output variables. Physiological conditions *in*
362 *vivo* deviate from these experimentally obtained states. Since kinetically-saturating
363 concentrations, *e.g.*, of ADP or oxygen, may not apply to physiological intracellular conditions,
364 relevant information is obtained in studies of kinetic responses to variations in [ADP], or of
365 respiratory capacities in the range between kinetically-saturating [O₂] and anoxia (Gnaiger
366 2001).

367 **The steady-state:** Mitochondria represent a thermodynamically open system in non-
368 equilibrium states of biochemical energy transformation. State variables (protonmotive force;
369 redox states) and metabolic *rates* (fluxes) are measured in defined mitochondrial respiratory
370 *states*. Steady-states can be obtained only in open systems, in which changes by *internal*
371 transformations, *e.g.*, O₂ consumption, are instantaneously compensated for by *external* fluxes,
372 *e.g.*, O₂ supply, preventing a change of oxygen concentration in the system (Gnaiger 1993b).
373 Mitochondrial respiratory states monitored in closed systems satisfy the criteria of pseudo-
374 steady states for limited periods of time, when changes in the system (concentrations of O₂, fuel
375 substrates, ADP, P_i, H⁺) do not exert significant effects on metabolic fluxes (respiration,
376 phosphorylation). Such pseudo-steady states require respiratory media with sufficient buffering
377 capacity and substrates maintained at kinetically-saturating concentrations, and thus depend on
378 the kinetics of the processes under investigation.

379 **Specification of biochemical dose:** Substrates, uncouplers, inhibitors, and other
380 biochemical reagents are titrated to dissect mitochondrial function. Nominal concentrations of
381 these substances are usually reported as initial amount of substance concentration [mol·L⁻¹] in
382 the incubation medium. When aiming at the measurement of kinetically saturated processes—
383 such as OXPHOS-capacities, the concentrations for substrates can be chosen according to the

384 apparent equilibrium constant, K_m' . In the case of hyperbolic kinetics, only 80% of maximum
 385 respiratory capacity is obtained at a substrate concentration of four times the K_m' , whereas
 386 substrate concentrations of 5, 9, 19 and 49 times the K_m' are theoretically required for reaching
 387 83%, 90%, 95% or 98% of the maximal rate (Gnaiger 2001). Other reagents are chosen to
 388 inhibit or alter some process. The amount of these chemicals in an experimental incubation is
 389 selected to maximize effect, yet not lead to unacceptable off-target consequences that would
 390 adversely affect the data being sought. Specifying the amount of substance in an incubation as
 391 nominal concentration in the aqueous incubation medium can be ambiguous (Doskey *et al.*
 392 2015), particularly when lipophilic substances (oligomycin; uncouplers, permeabilization
 393 agents) or cations (TPP⁺; fluorescent dyes such as safranin, TMRM) are applied which
 394 accumulate in biological membranes or the mitochondrial matrix. For example, a dose of
 395 digitonin of 8 fmol·cell⁻¹ (10 pg·cell⁻¹; 10 μg·10⁻⁶ cells) is optimal for permeabilization of
 396 endothelial cells, and the concentration in the incubation medium has to be adjusted according
 397 to the cell density applied (Doerrier *et al.* 2018). Generally, dose/exposure can be specified per
 398 unit of biological sample, *i.e.*, (nominal moles of xenobiotic)/(number of cells) [mol·cell⁻¹] or,
 399 as appropriate, per mass of biological sample [mol·kg⁻¹]. This approach to specification of
 400 dose/exposure provides a scalable parameter that can be used to design experiments, help
 401 interpret a wide variety of experimental results, and provide absolute information that allows
 402 researchers worldwide to make the most use of published data (Doskey *et al.* 2015).
 403



404
 405 **Fig. 2. The proton circuit and coupling in oxidative phosphorylation (OXPHOS).** 2[H]
 406 indicates the reduced hydrogen equivalents of fuel substrates of the catabolic reaction k with
 407 oxygen. Oxygen flux, J_{kO_2} , through the catabolic ET-pathway, is coupled to flux through the
 408 phosphorylation-pathway of ADP to ATP, $J_{P»}$. The proton pumps of the ET-pathway drive
 409 proton flux into the positive (pos) compartment, J_{mH^+pos} , generating the output protonmotive
 410 force (motive, subscript m). F-ATPase is coupled to inward proton current into the negative
 411 (neg) compartment, J_{mH^+neg} , to phosphorylate ADP+ P_i to ATP. The system defined by the
 412 boundaries (full black line) is not a black box, but is analysed as a compartmental system. The
 413 negative compartment (neg-compartment, enclosed by the dotted line) is the matrix space,
 414 separated by the mtIM from the positive compartment (pos-compartment). ADP+ P_i and ATP
 415 are the substrate- and product-compartments (scalar ADP and ATP compartments, D-comp.
 416 and T-comp.), respectively. At steady-state proton turnover, $J_{\infty H^+}$, and ATP turnover, $J_{\infty P}$,
 417 maintain concentrations constant, when $J_{mH^+} = J_{mH^+pos} = J_{mH^+neg}$, and $J_{P\infty} = J_{P»} = J_{P<}$. Modified
 418 from Gnaiger (2014).

419 **Phosphorylation, P \gg , and P \gg /O $_2$ ratio:** *Phosphorylation* in the context of OXPHOS is
 420 defined as phosphorylation of ADP by P $_i$ to ATP. On the other hand, the term phosphorylation
 421 is used generally in many contexts, *e.g.*, protein phosphorylation. This justifies consideration
 422 of a symbol more discriminating and specific than P as used in the P/O ratio (phosphate to
 423 atomic oxygen ratio), where P indicates phosphorylation of ADP to ATP or GDP to GTP. We
 424 propose the symbol P \gg for the endergonic (uphill) direction of phosphorylation ADP \rightarrow ATP,
 425 and likewise the symbol P \ll for the corresponding exergonic (downhill) hydrolysis ATP \rightarrow ADP
 426 (**Fig. 2**). P \gg refers mainly to electrontransfer phosphorylation but may also involve substrate-
 427 level phosphorylation as part of the tricarboxylic acid (TCA) cycle (succinyl-CoA ligase) and
 428 phosphorylation of ADP catalyzed by phosphoenolpyruvate carboxykinase.
 429 Transphosphorylation is performed by adenylate kinase, creatine kinase, hexokinase and
 430 nucleoside diphosphate kinase. In isolated mammalian mitochondria, ATP production
 431 catalyzed by adenylate kinase (2 ADP \leftrightarrow ATP + AMP) proceeds without fuel substrates in the
 432 presence of ADP (Komlódi and Tretter 2017). Kinase cycles are involved in intracellular energy
 433 transfer and signal transduction for regulation of energy flux.

434 The P \gg /O $_2$ ratio (P \gg /4 e $^-$) is two times the ‘P/O’ ratio (P \gg /2 e $^-$) of classical bioenergetics.
 435 P \gg /O $_2$ is a generalized symbol, independent phosphorylation assessment by determination of P $_i$
 436 consumption (P $_i$ /O $_2$ flux ratio), ADP depletion (ADP/O $_2$ flux ratio), or ATP production
 437 (ATP/O $_2$ flux ratio). The mechanistic P \gg /O $_2$ ratio—or P \gg /O $_2$ stoichiometry—is calculated from
 438 the proton-to-oxygen and proton-to-phosphorylation coupling stoichiometries (**Fig. 1A**),
 439

$$440 \quad P\gg/O_2 = \frac{H_{\text{pos}}^+/O_2}{H_{\text{neg}}^+/P\gg} \quad (1)$$

441
 442 The H $^+$ _{pos}/O $_2$ *coupling stoichiometry* (referring to the full 4 electron reduction of O $_2$) depends
 443 on the ET-pathway control state which defines the relative involvement of the three coupling
 444 sites (CI, CIII and CIV) in the catabolic pathway of electrons to O $_2$. This varies with: (1) a
 445 bypass of CI by single or multiple electron input into the Q-junction; and (2) a bypass of CIV
 446 by involvement of AOX. H $^+$ _{pos}/O $_2$ is 12 in the ET-pathways involving CIII and CIV as proton
 447 pumps, increasing to 20 for the NADH-pathway (**Fig. 1A**), but a general consensus on H $^+$ _{pos}/O $_2$
 448 stoichiometries remains to be reached (Hinkle 2005; Wikström and Hummer 2012; Sazanov
 449 2015). The H $^+$ _{neg}/P \gg coupling stoichiometry (3.7; **Fig. 1A**) is the sum of 2.7 H $^+$ _{neg} required by
 450 the F-ATPase of vertebrate and most invertebrate species (Watt *et al.* 2010) and the proton
 451 balance in the translocation of ADP, ATP and P $_i$ (**Fig. 1B**). Taken together, the mechanistic
 452 P \gg /O $_2$ ratio is calculated at 5.4 and 3.3 for NADH- and succinate-linked respiration, respectively
 453 (Eq. 1). The corresponding classical P \gg /O ratios (referring to the 2 electron reduction of 0.5 O $_2$)
 454 are 2.7 and 1.6 (Watt *et al.* 2010), in agreement with the measured P \gg /O ratio for succinate of
 455 1.58 \pm 0.02 (Gnaiger *et al.* 2000).

456 The effective P \gg /O $_2$ flux ratio ($Y_{P\gg/O_2} = J_{P\gg}/J_{kO_2}$) is diminished relative to the mechanistic
 457 P \gg /O $_2$ ratio by intrinsic and extrinsic uncoupling and dyscoupling (**Fig. 3**). Such generalized
 458 uncoupling is different from switching to mitochondrial pathways that involve fewer than three
 459 proton pumps (‘coupling sites’: Complexes CI, CIII and CIV), bypassing CI through multiple
 460 electron entries into the Q-junction, or CIII and CIV through AOX (**Fig. 1**). Reprogramming of
 461 mitochondrial pathways may be considered as a switch of gears (changing the stoichiometry)
 462 rather than uncoupling (loosening the stoichiometry). In addition, $Y_{P\gg/O_2}$ depends on several
 463 experimental conditions of flux control, increasing as a hyperbolic function of [ADP] to a
 464 maximum value (Gnaiger 2001).

465 **Control and regulation:** The terms metabolic *control* and *regulation* are frequently used
 466 synonymously, but are distinguished in metabolic control analysis: ‘We could understand the
 467 regulation as the mechanism that occurs when a system maintains some variable constant over
 468 time, in spite of fluctuations in external conditions (homeostasis of the internal state). On the

469 other hand, metabolic control is the power to change the state of the metabolism in response to
 470 an external signal' (Fell 1997). Respiratory control may be induced by experimental control
 471 signals that *exert* an influence on: (1) ATP demand and ADP phosphorylation-rate; (2) fuel
 472 substrate composition, pathway competition; (3) available amounts of substrates and oxygen,
 473 *e.g.*, starvation and hypoxia; (4) the protonmotive force, redox states, flux–force relationships,
 474 coupling and efficiency; (5) Ca²⁺ and other ions including H⁺; (6) inhibitors, *e.g.*, nitric oxide
 475 or intermediary metabolites such as oxaloacetate; (7) signalling pathways and regulatory
 476 proteins, *e.g.*, insulin resistance, transcription factor hypoxia inducible factor 1. *Mechanisms* of
 477 respiratory control and regulation include adjustments of: (1) enzyme activities by allosteric
 478 mechanisms and phosphorylation; (2) enzyme content, concentrations of cofactors and
 479 conserved moieties—such as adenylates, nicotinamide adenine dinucleotide [NAD⁺/NADH],
 480 coenzyme Q, cytochrome *c*); (3) metabolic channeling by supercomplexes; and (4)
 481 mitochondrial density (enzyme concentrations and membrane area) and morphology (cristae
 482 folding, fission and fusion). Mitochondria are targeted directly by hormones, thereby affecting
 483 their energy metabolism (Lee *et al.* 2013; Gerö and Szabo 2016; Price and Dai 2016; Moreno
 484 *et al.* 2017). Evolutionary or acquired differences in the genetic and epigenetic basis of
 485 mitochondrial function (or dysfunction) between subjects and gene therapy; age; gender,
 486 biological sex, and hormone concentrations; life style including exercise and nutrition; and
 487 environmental issues including thermal, atmospheric, toxicological and pharmacological
 488 factors, exert an influence on all control mechanisms listed above. For reviews, see Brown
 489 1992; Gnaiger 1993a, 2009; 2014; Paradies *et al.* 2014; Morrow *et al.* 2017.

490 **Respiratory control and response:** Lack of control by a metabolic pathway, *e.g.*,
 491 phosphorylation-pathway, means that there will be no response to a variable activating it, *e.g.*,
 492 [ADP]. The reverse, however, is not true as the absence of a response to [ADP] does not exclude
 493 the phosphorylation-pathway from having some degree of control. The degree of control of a
 494 component of the OXPHOS-pathway on an output variable—such as oxygen flux, will in
 495 general be different from the degree of control on other outputs—such as phosphorylation-flux
 496 or proton leak flux. Therefore, it is necessary to be specific as to which input and output are
 497 under consideration (Fell 1997).

498 **Respiratory coupling control and ET-pathway control:** Respiratory control refers to
 499 the ability of mitochondria to adjust oxygen consumption in response to external control signals
 500 by engaging various mechanisms of control and regulation. Respiratory control is monitored in
 501 a mitochondrial preparation under conditions defined as respiratory states. When
 502 phosphorylation of ADP to ATP is stimulated or depressed, an increase or decrease is observed
 503 in electron flux linked to oxygen consumption in respiratory coupling states of intact
 504 mitochondria ('controlled states' in the classical terminology of bioenergetics). Alternatively,
 505 coupling of electron transfer with phosphorylation is disengaged by disruption of the integrity
 506 of the mtIM or by uncouplers, functioning like a clutch in a mechanical system. The
 507 corresponding coupling control state is characterized by high levels of oxygen consumption
 508 without control by P» ('uncontrolled state').

509 ET-pathway control states are obtained in mitochondrial preparations by depletion of
 510 endogenous substrates and addition to the mitochondrial respiration medium of fuel substrates
 511 (CHNO; 2[H] in **Fig. 2**) and specific inhibitors, activating selected mitochondrial catabolic
 512 pathways, *k* (**Fig. 1**). Coupling control states and pathway control states are complementary,
 513 since mitochondrial preparations depend on an exogenous supply of pathway-specific fuel
 514 substrates and oxygen (Gnaiger 2014).

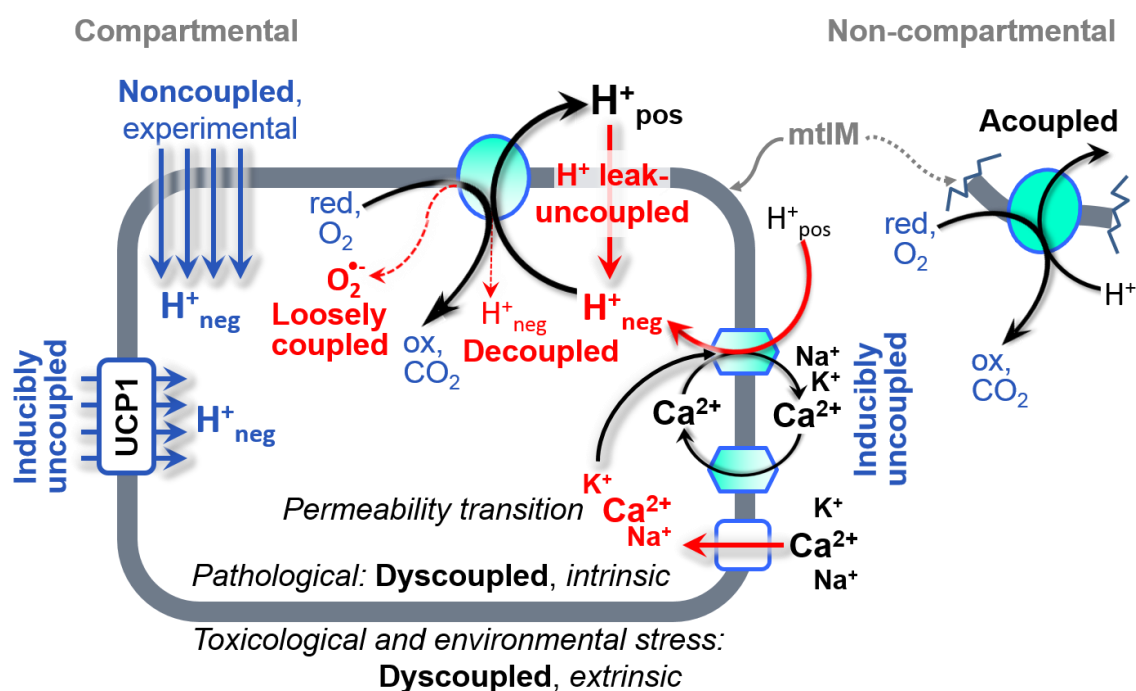
515 **Coupling:** In mitochondrial electron transfer (**Fig. 1**), vectorial transmembrane proton
 516 flux is coupled through the proton pumps CI, CIII and CIV to the catabolic flux of scalar
 517 reactions, collectively measured as oxygen flux (**Fig. 2**). Thus mitochondria are elements of
 518 energy transformation. Energy cannot be lost or produced in any internal process (First Law of
 519 thermodynamics). Open and closed systems can gain or loose energy only by external fluxes—

520 by exchange with the environment. Energy is a conserved quantity. Therefore, energy can
 521 neither be produced by mitochondria, nor is there any internal process without energy
 522 conservation. Exergy is defined as the ‘free energy’ with the potential to perform work.
 523 *Coupling* is the mechanistic linkage of an exergonic process (spontaneous, negative exergy
 524 change) with an endergonic process (positive exergy change) in energy transformations which
 525 conserve part of the exergy that would be irreversible lost or dissipated in an uncoupled process.

526 **Uncoupling:** Uncoupling of mitochondrial respiration is a general term comprising
 527 diverse mechanisms. Differences of terms—uncoupled *vs.* noncoupled—are easily overlooked,
 528 although they relate to different mechanisms of uncoupling (**Fig. 3**).

- 529 1. Proton leak across the mtIM from the pos- to the neg-compartment (**Fig. 2**);
- 530 2. Cycling of other cations, strongly stimulated by permeability transition;
- 531 3. Proton slip in the proton pumps when protons are effectively not pumped (CI, CIII and
 532 CIV) or are not driving phosphorylation (F-ATPase);
- 533 4. Loss of compartmental integrity when electron transfer is acoupled;
- 534 5. Electron leak in the loosely coupled univalent reduction of oxygen (O_2 ; dioxygen) to
 535 superoxide ($O_2^{\bullet -}$; superoxide anion radical).

536



537

538 **Fig 3. Mechanisms of respiratory uncoupling.** An intact mitochondrial inner membrane,
 539 mtIM, is required for vectorial, compartmental coupling. ‘Acoupled’ respiration is the
 540 consequence of structural disruption with catalytic activity of non-compartmental
 541 mitochondrial fragments. Inducibly uncoupled (activation of UCP1) and experimentally
 542 noncoupled respiration (titration of protonophores) stimulate respiration to maximum oxygen
 543 flux. H^+ leak-uncoupled, decoupled, and loosely coupled respiration are components of intrinsic
 544 uncoupling. Pathological dysfunction may affect all types of uncoupling, including
 545 permeability transition, causing intrinsically dyscoupled respiration. Similarly, toxicological
 546 and environmental stress factors can cause extrinsically dyscoupled respiration.

547

548 2.2. Coupling states and respiratory rates

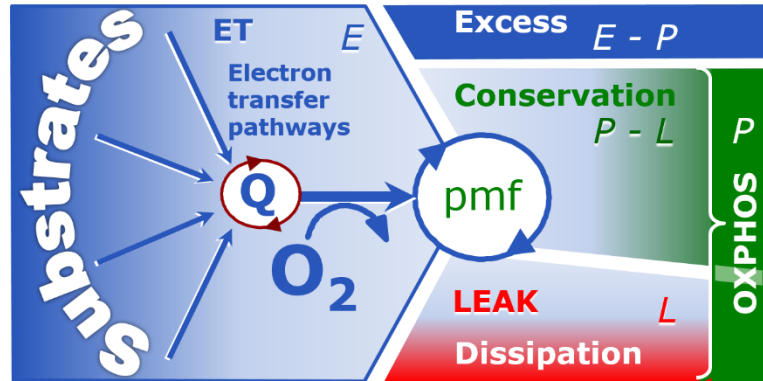
549

550 **Respiratory capacities in coupling control states:** To extend the classical nomenclature
 551 on mitochondrial coupling states (Section 2.3) by a concept-driven terminology that
 552 incorporates explicitly information on the nature of respiratory states, the terminology must be

553 general and not restricted to any particular experimental protocol or mitochondrial preparation
 554 (Gnaiger 2009). We focus primarily on the conceptual ‘why’, along with clarification of the
 555 experimental ‘how’. Respiratory capacities delineate, comparable to channel capacity in
 556 information theory (Schneider 2006), the upper bound of the rate of respiration measured in
 557 defined coupling control states and electron transfer-pathway (ET-pathway) states (Fig. 4).
 558

559 **Fig. 4. Four-compartment**
 560 **model of oxidative**

561 **phosphorylation.** Respiratory
 562 states (ET, OXPHOS, LEAK;
 563 **Table 1**) and corresponding rates
 564 (E , P , L) are connected by the
 565 protonmotive force, pmf. ET-
 566 capacity, E , is partitioned into (1)
 567 dissipative LEAK-respiration, L ,
 568 when the Gibbs energy change of
 569 catabolic O_2 consumption is



570 irreversibly lost, (2) net OXPHOS-capacity, $P-L$, with partial conservation of the capacity to
 571 perform work, and (3) the excess capacity, $E-P$. Modified from Gnaiger (2014).
 572

573 **Table 1. Coupling states and residual oxygen consumption in mitochondrial**
 574 **preparations in relation to respiration- and phosphorylation-rate, J_{kO_2} and $J_{P_{\gg}}$,**
 575 **and protonmotive force, pmf.** Coupling states are established at kinetically-
 576 saturating concentrations of fuel substrates and O_2 .

State	J_{kO_2}	$J_{P_{\gg}}$	Pmf	Inducing factors	Limiting factors
LEAK	L ; low, cation leak-dependent respiration	0	max.	proton leak, slip, and cation cycling	$J_{P_{\gg}} = 0$: (1) without ADP, L_N ; (2) max. ATP/ADP ratio, L_T ; or (3) inhibition of the phosphorylation-pathway, L_{Omy}
OXPHOS	P ; high, ADP-stimulated respiration	max.	High	kinetically-saturating [ADP] and $[P_i]$	$J_{P_{\gg}}$, by phosphorylation-pathway; or J_{kO_2} by ET-capacity
ET	E ; max., noncoupled respiration	0	Low	optimal external uncoupler concentration for max. $J_{O_2, E}$	J_{kO_2} by ET-capacity
ROX	R_{ox} ; min., residual O_2 consumption	0	0	$J_{O_2, Rox}$ in non-ET-pathway oxidation reactions	full inhibition of ET-pathway; or absence of fuel substrates

577
 578 To provide a diagnostic reference for respiratory capacities of core energy metabolism,
 579 the capacity of *oxidative phosphorylation*, OXPHOS, is measured at kinetically-saturating
 580 concentrations of ADP and P_i . The *oxidative* ET-capacity reveals the limitation of OXPHOS-
 581 capacity mediated by the *phosphorylation*-pathway. The ET- and phosphorylation-pathways
 582 comprise coupled segments of the OXPHOS-system. ET-capacity is measured as noncoupled
 583 respiration by application of *external uncouplers*. The contribution of *intrinsically uncoupled*

584 oxygen consumption is studied in the absence of ADP—by not stimulating phosphorylation, or
 585 by inhibition of the phosphorylation-pathway. The corresponding states are collectively
 586 classified as LEAK-states, when oxygen consumption compensates mainly for ion leaks,
 587 including the proton leak. Defined coupling states are induced by: (1) adding cation chelators
 588 such as EGTA, binding free Ca^{2+} and thus limiting cation cycling; (2) adding ADP and P_i ; (3)
 589 inhibiting the phosphorylation-pathway; and (4) uncoupler titrations, while maintaining a
 590 defined ET-pathway state with constant fuel substrates and inhibitors of specific branches of
 591 the ET-pathway (**Fig. 1**).

592 The three coupling states, ET, LEAK and OXPHOS, are shown schematically with the
 593 corresponding respiratory rates, abbreviated as E , L and P , respectively (**Fig. 4**). We distinguish
 594 metabolic *pathways* from metabolic *states* and the corresponding metabolic *rates*; for example:
 595 ET-pathways (**Fig. 4**), ET-state (**Fig. 5C**), and ET-capacity, E , respectively (**Table 1**). The
 596 protonmotive force is *high* in the OXPHOS-state when it drives phosphorylation, *maximum* in
 597 the LEAK-state of coupled mitochondria, driven by LEAK-respiration at a minimum back flux
 598 of cations to the matrix side, and *very low* in the ET-state when uncouplers short-circuit the
 599 proton cycle (**Table 1**).

600 E may exceed or be equal to P . $E > P$ is observed in many types of mitochondria, varying
 601 between species, tissues and cell types (Gnaiger 2009). $E - P$ is the excess ET-capacity pushing
 602 the phosphorylation-flux (**Fig. 1B**) to the limit of its *capacity of utilizing* the protonmotive force.
 603 In addition, the magnitude of $E - P$ depends on the tightness of respiratory coupling or degree of
 604 uncoupling, since an increase of L causes P to increase towards the limit of E . The *excess* $E - P$
 605 capacity, $E - P$, therefore, provides a sensitive diagnostic indicator of specific injuries of the
 606 phosphorylation-pathway, under conditions when E remains constant but P declines relative to
 607 controls (**Fig. 4**). Substrate cocktails supporting simultaneous convergent electron transfer to
 608 the Q-junction for reconstitution of TCA cycle function establish pathway control states with
 609 high ET-capacity, and consequently increase the sensitivity of the $E - P$ assay.

610 E cannot theoretically be lower than P . $E < P$ must be discounted as an artefact, which
 611 may be caused experimentally by: (1) loss of oxidative capacity during the time course of the
 612 respirometric assay, since E is measured subsequently to P ; (2) using insufficient uncoupler
 613 concentrations; (3) using high uncoupler concentrations which inhibit ET (Gnaiger 2008); (4)
 614 high oligomycin concentrations applied for measurement of L before titrations of uncoupler,
 615 when oligomycin exerts an inhibitory effect on E . On the other hand, the excess ET-capacity is
 616 overestimated if non-saturating $[\text{ADP}]$ or $[\text{P}_i]$ are used. See State 3 in the next section.

617 The net OXPHOS-capacity is calculated by subtracting L from P (**Fig. 4**). Then the net
 618 $P \gg \text{O}_2$ equals $P \gg (P - L)$, wherein the dissipative LEAK component in the OXPHOS-state may
 619 be overestimated. This can be avoided by measuring LEAK-respiration in a state when the
 620 protonmotive force is adjusted to its slightly lower value in the OXPHOS-state—by titration of
 621 an ET inhibitor (Divakaruni and Brand 2011). Any turnover-dependent components of proton
 622 leak and slip, however, are underestimated under these conditions (Garlid *et al.* 1993). In
 623 general, it is inappropriate to use the term *ATP production* or *ATP turnover* for the difference
 624 of oxygen consumption measured in states P and L . The difference $P - L$ is the upper limit of the
 625 part of OXPHOS-capacity that is freely available for ATP production (corrected for LEAK-
 626 respiration) and is fully coupled to phosphorylation with a maximum mechanistic stoichiometry
 627 (**Fig. 4**).

628 **LEAK-state (Fig. 5A):** The LEAK-state is defined as a state of mitochondrial respiration
 629 when O_2 flux mainly compensates for ion leaks in the absence of ATP synthesis, at kinetically-
 630 saturating concentrations of O_2 and respiratory fuel substrates. LEAK-respiration is measured
 631 to obtain an estimate of *intrinsic uncoupling* without addition of an experimental uncoupler: (1)

632 in the absence of adenylates; (2)
 633 after depletion of ADP at a
 634 maximum ATP/ADP ratio; or (3)
 635 after inhibition of the
 636 phosphorylation-pathway
 637 by inhibitors of F-ATPase—such as
 638 oligomycin, or of adenine
 639 nucleotide translocase—such as
 640 carboxyatractyloside.

641 Adjustment of the nominal
 642 concentration of these inhibitors
 643 to the density of biological
 644 sample applied can minimize or
 645 avoid inhibitory side-effects
 646 exerted on ET-capacity or even
 647 some dyscoupling.

648 **Proton leak and**
 649 **uncoupled respiration:** Proton
 650 leak is a leak current of protons.
 651 The intrinsic proton leak is the
 652 *uncoupled* process in which
 653 protons diffuse across the mtIM
 654 in the dissipative direction of the
 655 downhill protonmotive force
 656 without coupling to
 657 phosphorylation (Fig. 5A). The
 658 proton leak flux depends non-
 659 linearly on the protonmotive
 660 force (Garlid *et al.* 1989;
 661 Divakaruni and Brand 2011), it is
 662 a property of the mtIM and may
 663 be enhanced due to possible
 664 contaminations by free fatty
 665 acids. Inducible uncoupling
 666 mediated by uncoupling protein
 667 1 (UCP1) is physiologically
 668 controlled, *e.g.*, in brown
 669 adipose tissue. UCP1 is a
 670 member of the mitochondrial
 671 carrier family which is involved
 672 in the translocation of protons
 673 across the mtIM (Klingenberg
 674 2017). Consequently, the short-
 675 circuit diminishes the protonmotive
 676 force and stimulates electron transfer to O₂ and heat
 677 dissipation without phosphorylation of ADP.

677 **Cation cycling:** There can be other cation contributors to leak current including calcium
 678 and probably magnesium. Calcium current is balanced by mitochondrial Na⁺/Ca²⁺ exchange,
 679 which is balanced by Na⁺/H⁺ or K⁺/H⁺ exchanges. This is another effective uncoupling
 680 mechanism different from proton leak.
 681

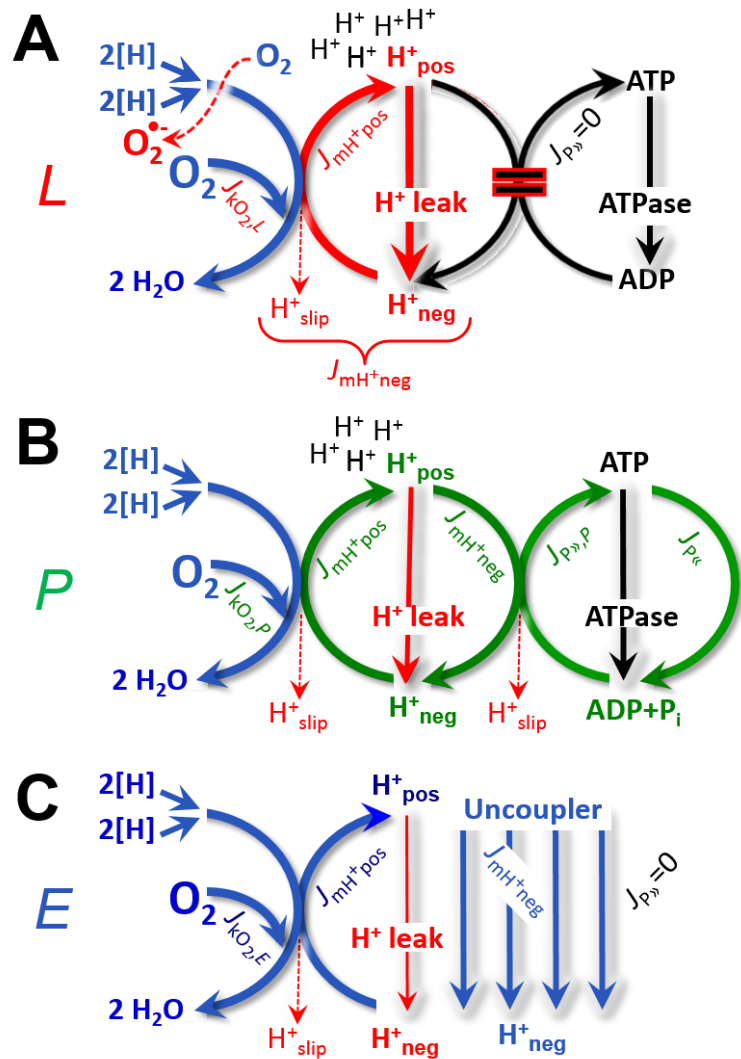


Fig. 5. Respiratory coupling states. A: LEAK-state and rate, L: Phosphorylation is arrested, $J_{P>} = 0$, and catabolic oxygen flux, $J_{kO_2,L}$, is controlled mainly by the proton leak, $J_{mH^+neg,L}$, at maximum protonmotive force (Fig. 3). **B: OXPHOS-state and rate, P:** Phosphorylation, $J_{P>}$, is stimulated by kinetically-saturating [ADP] and [P_i], and is supported by a high protonmotive force. O₂ flux, $J_{kO_2,P}$, is well-coupled at a $P>/O_2$ ratio of $J_{P>,P}/J_{O_2,P}$. **C: ET-state and rate, E:** Noncoupled respiration, $J_{kO_2,E}$, is maximum at optimum exogenous uncoupler concentration and phosphorylation is zero, $J_{P>} = 0$. See also Fig. 2.

682 **Table 2. Distinction of terms related to respiratory coupling and uncoupling**
 683 **(Fig. 3).**

Term	$J_{\text{K}O_2}$	$P \gg O_2$	Note	
acoupled		0	electron transfer in mitochondrial fragments without vectorial proton translocation	
uncoupled	L	0	non-phosphorylating LEAK-respiration	
intrinsic, no protonophore added	ion leak uncoupled	0	component of LEAK-respiration, uncoupled <i>sui generis</i> , ion diffusion across the mtIM	
		0	component of LEAK-respiration, proton slip	
		0	component of LEAK-respiration, lower coupling due to superoxide formation and bypass of proton pumps	
	dyscoupled	0	pathologically, toxicologically, environmentally increased uncoupling, mitochondrial dysfunction	
	inducibly uncoupled	E	0	by UCPI or cation (<i>e.g.</i> , Ca^{2+}) cycling
	noncoupled	E	0	non-phosphorylating respiration stimulated to maximum flux at optimum exogenous uncoupler concentration (Fig. 5C)
well-coupled	P	high	phosphorylating respiration with an intrinsic LEAK component (Fig. 5B)	
fully coupled	$P - L$	max.	OXPHOS-capacity corrected for LEAK-respiration (Fig. 4)	

684
 685 **Proton slip and decoupled respiration:** Proton slip is the *decoupled* process in which
 686 protons are only partially translocated by a proton pump of the ET-pathways and slip back to
 687 the original compartment. The proton leak is the dominant contributor to the overall leak current
 688 in mammalian mitochondria incubated under physiological conditions at 37 °C, whereas proton
 689 slip is increased at lower experimental temperature (Canton *et al.* 1995). Proton slip can also
 690 happen in association with the F-ATPase, in which the proton slips downhill across the pump
 691 to the matrix without contributing to ATP synthesis. In each case, proton slip is a property of
 692 the proton pump and increases with the pump turnover rate.

693 **Electron leak and loosely coupled respiration:** Superoxide production by the ETS leads
 694 to a bypass of proton pumps and correspondingly lower $P \gg O_2$ ratio. This depends on the actual
 695 site of electron leak and the scavenging of hydrogen peroxide by cytochrome *c*, whereby
 696 electrons may re-enter the ETS with proton translocation by CIV.

697 **Loss of compartmental integrity and acoupled respiration:** Electron transfer and O_2
 698 consumption proceed without compartmental proton translocation in disrupted mitochondrial
 699 fragments. Such fragments form during mitochondrial isolation, and may not fully fuse to re-
 700 establish structurally intact mitochondria. Loss of mtIM integrity, therefore, is the cause of
 701 acoupled respiration, which is a nonvectorial dissipative process without control by the
 702 protonmotive force.

703 **Dyscoupled respiration:** Mitochondrial injuries may lead to *dyscoupling* as a
 704 pathological or toxicological cause of *uncoupled* respiration. Dyscoupling may involve any
 705 type of uncoupling mechanism, *e.g.*, opening the permeability transition pore. Dyscoupled
 706 respiration is distinguished from the experimentally induced *noncoupled* respiration in the ET-
 707 state (**Fig. 3**).

708 **OXPHOS-state (Fig. 5B):** The OXPHOS-state is defined as the respiratory state with
 709 kinetically-saturating concentrations of O₂, respiratory and phosphorylation substrates, and
 710 absence of exogenous uncoupler, which provides an estimate of the maximal respiratory
 711 capacity in the OXPHOS-state for any given ET-pathway state. Respiratory capacities at
 712 kinetically-saturating substrate concentrations provide reference values or upper limits of
 713 performance, aiming at the generation of data sets for comparative purposes. Physiological
 714 activities and effects of substrate kinetics can be evaluated relative to the OXPHOS-capacity.

715 As discussed previously, 0.2 mM ADP does not fully saturate flux in isolated
 716 mitochondria (Gnaiger 2001; Puchowicz *et al.* 2004); greater ADP concentration is required,
 717 particularly in permeabilized muscle fibres and cardiomyocytes, to overcome limitations by
 718 intracellular diffusion and by the reduced conductance of the mtOM (Jepihhina *et al.* 2011,
 719 Illaste *et al.* 2012, Simson *et al.* 2016), either through interaction with tubulin (Rostovtseva *et al.*
 720 2008) or other intracellular structures (Birkedal *et al.* 2014). In permeabilized muscle fibre
 721 bundles of high respiratory capacity, the apparent K_m for ADP increases up to 0.5 mM (Saks *et al.*
 722 1998), consistent with experimental evidence that >90% saturation is reached only at >5
 723 mM ADP (Pesta and Gnaiger 2012). Similar ADP concentrations are also required for accurate
 724 determination of OXPHOS-capacity in human clinical cancer samples and permeabilized cells
 725 (Klepinin *et al.* 2016; Koit *et al.* 2017). Whereas 2.5 to 5 mM ADP is sufficient to obtain the
 726 actual OXPHOS-capacity in many types of permeabilized tissue and cell preparations,
 727 experimental validation is required in each specific case.

728 **Electron transfer-state (Fig. 5C):** The ET-state is defined as the *noncoupled* state with
 729 kinetically-saturating concentrations of O₂, respiratory substrate and optimum *exogenous*
 730 uncoupler concentration for maximum O₂ flux, as an estimate of ET-capacity. Inhibition of
 731 respiration is observed at higher than optimum uncoupler concentrations. As a consequence of
 732 the nearly collapsed protonmotive force, the driving force is insufficient for phosphorylation,
 733 and $J_{P_s} = 0$.

734 **ROX state and *Rox*:** Besides the three fundamental coupling states of mitochondrial
 735 preparations, the state of residual oxygen consumption, ROX, is relevant to assess respiratory
 736 function. ROX is not a coupling state. The rate of residual oxygen consumption, *Rox*, is defined
 737 as O₂ consumption due to oxidative side reactions remaining after inhibition of ET—with
 738 rotenone, malonic acid and antimycin A. Cyanide and azide not only inhibit CIV but also
 739 several peroxidases involved in *Rox*. ROX represents a baseline that is used to correct
 740 mitochondrial respiration in defined coupling states. *Rox* is not necessarily equivalent to non-
 741 mitochondrial respiration, considering oxygen-consuming reactions in mitochondria not related
 742 to ET—such as oxygen consumption in reactions catalyzed by monoamine oxidases (type A
 743 and B), monooxygenases (cytochrome P450 monooxygenases), dioxygenase (sulfur
 744 dioxygenase and trimethyllysine dioxygenase), and several hydroxylases. Mitochondrial
 745 preparations, especially those obtained from liver, may be contaminated by peroxisomes. This
 746 fact makes the exact determination of mitochondrial oxygen consumption and mitochondria-
 747 associated generation of reactive oxygen species complicated (Schönfeld *et al.* 2009). The
 748 dependence of ROX-linked oxygen consumption needs to be studied in detail together with
 749 non-ET enzyme activities, availability of specific substrates, oxygen concentration, and
 750 electron leakage leading to the formation of reactive oxygen species.

751 2.3. Classical terminology for isolated mitochondria

752 *'When a code is familiar enough, it ceases appearing like a code; one forgets that there*
 753 *is a decoding mechanism. The message is identical with its meaning'* (Hofstadter 1979).

754
 755
 756 Chance and Williams (1955; 1956) introduced five classical states of mitochondrial respiration
 757 and cytochrome redox states. **Table 3** shows a protocol with isolated mitochondria in a closed

758 respirometric chamber, defining a sequence of respiratory states. States and rates are not
759 specifically distinguished in this nomenclature.

760

761

762

763

Table 3. Metabolic states of mitochondria (Chance and Williams, 1956; Table V).

State	[O ₂]	ADP level	Substrate Level	Respiration rate	Rate-limiting substance
1	>0	low	low	slow	ADP
2	>0	high	~0	slow	substrate
3	>0	high	high	fast	respiratory chain
4	>0	low	high	slow	ADP
5	0	high	high	0	oxygen

764

765

766

767

768

769

770

771

772

773

774

775

776

777

778

779

780

781

782

783

784

785

786

787

788

789

790

791

792

793

794

795

796

797

798

799

800

801

State 1 is obtained after addition of isolated mitochondria to air-saturated isoosmotic/isotonic respiration medium containing P_i, but no fuel substrates and no adenylates, *i.e.*, AMP, ADP, ATP.

State 2 is induced by addition of a ‘high’ concentration of ADP (typically 100 to 300 μM), which stimulates respiration transiently on the basis of endogenous fuel substrates and phosphorylates only a small portion of the added ADP. State 2 is then obtained at a low respiratory activity limited by exhausted endogenous fuel substrate availability (**Table 3**). If addition of specific inhibitors of respiratory complexes—such as rotenone—does not cause a further decline of oxygen consumption, State 2 is equivalent to the state of residual oxygen consumption, ROX (See below.). If inhibition is observed, undefined endogenous fuel substrates are a confounding factor of pathway control, contributing to the effect of subsequently externally added substrates and inhibitors. In contrast to the original protocol, an alternative sequence of titration steps is frequently applied, in which the alternative ‘State 2’ has an entirely different meaning, when this second state is induced by addition of fuel substrate without ADP (LEAK-state; in contrast to State 2 defined in **Table 1** as a ROX state), followed by addition of ADP.

State 3 is the state stimulated by addition of fuel substrates while the ADP concentration is still high (**Table 3**) and supports coupled energy transformation through oxidative phosphorylation. ‘High ADP’ is a concentration of ADP specifically selected to allow the measurement of State 3 to State 4 transitions of isolated mitochondria in a closed respirometric chamber. Repeated ADP titration re-establishes State 3 at ‘high ADP’. Starting at oxygen concentrations near air-saturation (ca. 200 μM O₂ at sea level and 37 °C), the total ADP concentration added must be low enough (typically 100 to 300 μM) to allow phosphorylation to ATP at a coupled rate of oxygen consumption that does not lead to oxygen depletion during the transition to State 4. In contrast, kinetically-saturating ADP concentrations usually are 10-fold higher than ‘high ADP’, *e.g.*, 2.5 mM in isolated mitochondria. The abbreviation State 3u is occasionally used in bioenergetics, to indicate the state of respiration after titration of an uncoupler, without sufficient emphasis on the fundamental difference between OXPHOS-capacity (*well-coupled* with an *endogenous* uncoupled component) and ET-capacity (*noncoupled*).

State 4 is a LEAK-state that is obtained only if the mitochondrial preparation is intact and well-coupled. Depletion of ADP by phosphorylation to ATP leads to a decline in the rate of oxygen consumption in the transition from State 3 to State 4. Under these conditions of State 4, a maximum protonmotive force and high ATP/ADP ratio are maintained. For calculation of P_»/O₂ ratios the gradual decline of Y_{P_»/O₂} towards diminishing [ADP] at State 4 must be taken into account (Gnaiger 2001). State 4 respiration, L_T (**Table 1**), reflects intrinsic proton leak and intrinsic ATP hydrolysis activity. Oxygen consumption in State 4 is an overestimation of

802 LEAK-respiration if the contaminating ATP hydrolysis activity recycles some ATP to ADP,
 803 $J_{P\ll}$, which stimulates respiration coupled to phosphorylation, $J_{P\gg} > 0$. This can be tested by
 804 inhibition of the phosphorylation-pathway using oligomycin, ensuring that $J_{P\gg} = 0$ (State 4o).
 805 Alternatively, sequential ADP titrations re-establish State 3, followed by State 3 to State 4
 806 transitions while sufficient oxygen is available. Anoxia may be reached, however, before
 807 exhaustion of ADP (State 5).

808 **State 5** is the state after exhaustion of oxygen in a closed respirometric chamber.
 809 Diffusion of oxygen from the surroundings into the aqueous solution may be a confounding
 810 factor preventing complete anoxia (Gnaiger 2001). Chance and Williams (1955) provide an
 811 alternative definition of State 5, which gives it the different meaning of ROX versus anoxia:
 812 ‘State 5 may be obtained by antimycin A treatment or by anaerobiosis’.

813 In **Table 3**, only States 3 and 4 (and ‘State 2’ in the alternative protocol: addition of fuel
 814 substrates without ADP; not included in the table) are coupling control states, with the
 815 restriction that O_2 flux in State 3 may be limited kinetically by non-saturating ADP
 816 concentrations (**Table 1**).

817
 818

819 3. Normalization: fluxes and flows

820
 821
 822

823 3.1. Normalization: system or sample

824 The term *rate* is not sufficiently defined to be useful for a database (**Fig. 6**). The
 825 inconsistency of the meanings of rate becomes fully apparent when considering Galileo
 826 Galilei’s famous principle, that ‘bodies of different weight all fall at the same rate (have a
 827 constant acceleration)’ (Coopersmith 2010).

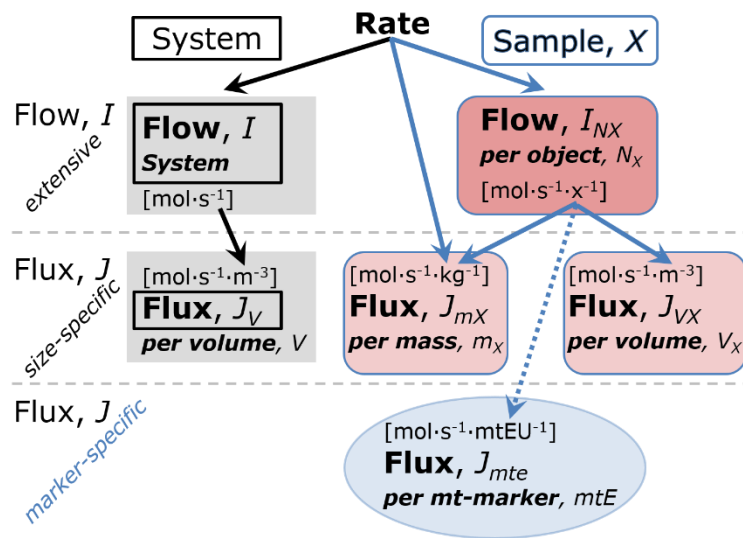
827

828 **Fig. 6. Different meanings of rate may lead to confusion, if the normalization is not**
 829 **sufficiently specified.** Results are frequently expressed as mass-
 830 specific *flux*, J_{mX} , per mg protein, dry or wet weight (mass). Cell
 831 volume, V_{cell} , may be used for normalization (volume-specific
 832 flux, J_{Vcell}), which must be clearly distinguished from flow per cell,
 833 I_{Ncell} , or flux, J_V , expressed for methodological reasons per
 834 volume of the measurement system. For details see **Table 4**.

843

844 **Flow per system, I :** In a generalization of electrical terms, flow as an extensive quantity
 845 (per system) is distinguished from flux as a size-specific quantity (per system size) (**Fig. 6**).
 846 Electric current is flow, I_{el} [$A \equiv C \cdot s^{-1}$] per system (extensive quantity). When dividing this
 847 extensive quantity by system size (cross-sectional area of a ‘wire’), a size-specific quantity is
 848 obtained, which is flux (current density), J_{el} [$A \cdot m^{-2} = C \cdot s^{-1} \cdot m^{-2}$].

849 **Extensive quantities:** An extensive quantity increases proportionally with system size.
 850 The magnitude of an extensive quantity is completely additive for non-interacting
 851 subsystems—such as mass or flow expressed per defined system. The magnitude of these
 852 quantities depends on the extent or size of the system (Cohen *et al.* 2008).



853 **Size-specific quantities:** ‘The adjective *specific* before the name of an extensive quantity
 854 is often used to mean *divided by mass*’ (Cohen *et al.* 2008). In this system-paradigm, mass-
 855 specific flux is flow divided by mass of the *system* (the total mass of everything within the
 856 measuring chamber). A mass-specific quantity is independent of the extent of non-interacting
 857 homogenous subsystems. Tissue-specific quantities (related to the *sample* in contrast to the
 858 *system*) are of fundamental interest in comparative mitochondrial physiology, where *specific*
 859 refers to the *type of the sample* rather than *mass of the system*. The term *specific*, therefore, must
 860 be clarified; *sample-specific*, *e.g.*, muscle mass-specific normalization, is distinguished from
 861 *system-specific* (mass or volume) quantities (**Fig. 6**).
 862

863 **Box 2: Metabolic fluxes and flows: vectorial and scalar**

864
 865 Fluxes are *vectors*, if they have *spatial* direction in addition to magnitude. A vector flux
 866 (surface-density of flow) is expressed per unit cross-sectional area, A [m^2], perpendicular to the
 867 direction of flux. *Flows* are defined as extensive quantities of the *system*, as vector or scalar
 868 flow, I or I [$\text{mol}\cdot\text{s}^{-1}$], respectively, then the corresponding vector and scalar *fluxes* are $J = I\cdot A^{-1}$
 869 [$\text{mol}\cdot\text{s}^{-1}\cdot\text{m}^{-2}$] and $J = I\cdot V^{-1}$ [$\text{mol}\cdot\text{s}^{-1}\cdot\text{m}^{-3}$], respectively, expressing flux as an area-specific vector
 870 or volume-specific scalar quantity. We suggest to define: (1) *vectorial* fluxes, which analyze
 871 translocations in continuous systems as functions of gradients; (2) *vectorial* fluxes, which
 872 describe translocations in discontinuous systems and are restricted to information on
 873 compartmental differences (**Fig. 2**, transmembrane proton flux); and (3) *scalar* fluxes, which
 874 are transformations in a homogenous system (**Fig. 2**, catabolic O_2 flux, J_{kO_2} [$\text{mol}\cdot\text{s}^{-1}\cdot\text{m}^{-3}$]).

875 Vectorial transmembrane proton fluxes, $J_{\text{mH}^+\text{pos}}$ and $J_{\text{mH}^+\text{neg}}$, are analyzed in a
 876 heterogenous compartmental system as a quantity with *directional* but not *spatial* information.
 877 Translocation of protons across the mtIM has a defined direction, either from the negative
 878 compartment (matrix space; negative, neg–compartment) to the positive compartment (inter-
 879 membrane space; positive, pos–compartment) or *vice versa* (**Fig. 2**). The arrows defining the
 880 direction of the translocation between the two compartments may point upwards or downwards,
 881 right or left, without any implication that these are actual directions in space. The pos–
 882 compartment is neither above nor below the neg–compartment in a spatial sense, but can be
 883 visualized arbitrarily in a figure in the upper position (**Fig. 2**). In general, the *compartmental*
 884 *direction* of vectorial translocation from the neg–compartment to the pos–compartment is
 885 defined by assigning the initial and final state as *ergodynamic compartments*, $\text{H}^+_{\text{neg}} \rightarrow \text{H}^+_{\text{pos}}$ or
 886 $0 = -1 \text{H}^+_{\text{neg}} + 1 \text{H}^+_{\text{pos}}$, related to work (erg = work) that must be performed to lift the proton from
 887 a lower to a higher electrochemical potential or from the lower to the higher ergodynamic
 888 compartment (Gnaiger 1993b).

889 In direct analogy to *vectorial* translocation, the direction of a *scalar* chemical reaction, A
 890 $\rightarrow B$ or $0 = -1 A + 1 B$, is defined by assigning substrates and products, A and B , as ergodynamic
 891 compartments. O_2 is defined as a substrate in respiratory O_2 consumption, which together with
 892 the fuel substrates comprises the substrate compartment of the catabolic reaction (**Fig. 2**).
 893 Volume-specific scalar O_2 flux is coupled to vectorial translocation, yielding the $\text{H}^+_{\text{pos}}/\text{O}_2$ ratio
 894 (**Fig. 1**).
 895

896 3.2. Normalization for system-size: flux per chamber volume

897
 898 **System-specific flux, J :** The experimental system (the experimental chamber) is part of
 899 the measurement apparatus, separated from the environment as an isolated, closed, open,
 900 isothermal or non-isothermal system (**Table 4**). On another level, we distinguish between (1)
 901 the *system* with volume V and mass m defined by the system boundaries, and (2) the *sample* or
 902 *objects* with volume V_X and mass m_X which are enclosed in the experimental chamber (**Fig. 6**).
 903 Metabolic O_2 flow per object, I_{X,O_2} , increases as the mass of the object is increased. Object mass-

904 specific O₂ flux, J_{mX,O_2} should be independent of the mass of the object studied in the instrument
 905 chamber, but system volume-specific O₂ flux, J_{V,O_2} (per volume of the instrument chamber),
 906 should increase in direct proportion to the mass of the object in the chamber. J_{V,O_2} depends on
 907 mass-concentration of the sample in the chamber, but should be independent of the chamber
 908 (system) volume. There are practical limitations to increase the mass-concentration of the
 909 sample in the chamber, when one is concerned about crowding effects and instrumental time
 910 resolution.

911 When the reactor volume does not change during the reaction, which is typical for liquid
 912 phase reactions, the volume-specific flux of a chemical reaction r is the time derivative of the
 913 advancement of the reaction per unit volume, $J_{V,rB} = d_r\zeta_B/dt \cdot V^{-1}$ [(mol·s⁻¹)·L⁻¹]. The rate of
 914 concentration change is dc_B/dt [(mol·L⁻¹)·s⁻¹], where concentration is $c_B = n_B/V$. There is a
 915 difference between (1) J_{V,rO_2} [mol·s⁻¹·L⁻¹] and (2) rate of concentration change [mol·L⁻¹·s⁻¹].
 916 These merge to a single expression only in closed systems. In open systems, external fluxes
 917 (such as O₂ supply) are distinguished from internal transformations (metabolic flux, O₂
 918 consumption). In a closed system, external flows of all substances are zero and O₂ consumption
 919 (internal flow of catabolic reactions k), I_{kO_2} [pmol·s⁻¹], causes a decline of the amount of O₂ in
 920 the system, n_{O_2} [nmol]. Normalization of these quantities for the volume of the system, V [L \equiv
 921 dm³], yields volume-specific O₂ flux, $J_{V,kO_2} = I_{kO_2}/V$ [nmol·s⁻¹·L⁻¹], and O₂ concentration, [O₂]
 922 or $c_{O_2} = n_{O_2}/V$ [μ mol·L⁻¹ = μ M = nmol·mL⁻¹]. Instrumental background O₂ flux is due to external
 923 flux into a non-ideal closed respirometer; then total volume-specific flux has to be corrected for
 924 instrumental background O₂ flux—O₂ diffusion into or out of the instrumental chamber. J_{V,kO_2}
 925 is relevant mainly for methodological reasons and should be compared with the accuracy of
 926 instrumental resolution of background-corrected flux, e.g., ± 1 nmol·s⁻¹·L⁻¹ (Gnaiger 2001).
 927 ‘Metabolic’ or catabolic indicates O₂ flux, J_{kO_2} , corrected for: (1) instrumental background O₂
 928 flux; (2) chemical background O₂ flux due to autoxidation of chemical components added to
 929 the incubation medium; and (3) *Rox* for O₂-consuming side reactions unrelated to the catabolic
 930 pathway k .

931 3.3. Normalization: per sample

932 The challenges of measuring mitochondrial respiratory flux are matched by those of
 933 normalization. Application of common and defined units is required for direct transfer of
 934 reported results into a database. The second [s] is the *SI* unit for the base quantity *time*. It is also
 935 the standard time-unit used in solution chemical kinetics. A rate may be considered as the
 936 numerator and normalization as the complementary denominator, which are tightly linked in
 937 reporting the measurements in a format commensurate with the requirements of a database.
 938 Normalization (Table 4) is guided by physicochemical principles, methodological
 939 considerations, and conceptual strategies (Fig. 7).

940 **Sample concentration, C_{mX} :** Normalization for sample concentration is required to
 941 report respiratory data. Considering a tissue or cells as the sample, X , the sample mass is m_X
 942 [mg] from which a mitochondrial preparation is obtained. m_X is frequently measured as wet or
 943 dry weight, W_w or W_d [mg], or as amount of tissue or cell protein, m_{Protein} . In the case of
 944 permeabilized tissues, cells, and homogenates, the sample concentration, $C_{mX} = m_X/V$ [mg·mL⁻¹
 945 = g·L⁻¹], is simply the mass of the subsample of tissue that is transferred into the instrument
 946 chamber.

947 **Mass-specific flux, J_{mX,O_2} :** Mass-specific flux is obtained by expressing respiration per
 948 mass of sample, m_X [mg]. X is the type of sample—tissue homogenate, permeabilized fibres or
 949 cells. Volume-specific flux is divided by mass concentration of X , $J_{mX,O_2} = J_{V,O_2}/C_{mX}$; or flow
 950 per cell is divided by mass per cell, $J_{m\text{cell},O_2} = I_{\text{cell},O_2}/M_{\text{cell}}$. If mass-specific O₂ flux is constant
 951 and independent of sample size (expressed as mass), then there is no interaction between the
 952 subsystems. A 1.5 mg and a 3.0 mg muscle sample respire at identical mass-specific flux.
 953
 954

955 Mass-specific O₂ flux, however, may change with the mass of a tissue sample, cells or isolated
 956 mitochondria in the measuring chamber, in which the nature of the interaction becomes an issue.
 957 Therefore, cell density must be optimization, particularly in experiments carried out in wells,
 958 considering the confluency of the cell monolayer or clumps of cells (Salabei *et al.* 2014).
 959

960 **Table 4. Sample concentrations and normalization of flux.**
 961

Expression	Symbol	Definition	Unit	Notes
Sample				
identity of sample	X	object: cell, tissue, animal, patient		
number of sample entities X	N_X	number of objects	x	
mass of sample X	m_X		kg	1
mass of object X	M_X	$M_X = m_X \cdot N_X^{-1}$	kg·x ⁻¹	1
Mitochondria				
mitochondria	mt	$X = \text{mt}$		
amount of mt-elements	mtE	quantity of mt-marker	mtEU	
Concentrations				
object number concentration	C_{NX}	$C_{NX} = N_X \cdot V^{-1}$	x·m ⁻³	2
sample mass concentration	C_{mX}	$C_{mX} = m_X \cdot V^{-1}$	kg·m ⁻³	
mitochondrial concentration	C_{mtE}	$C_{mtE} = mtE \cdot V^{-1}$	mtEU·m ⁻³	3
specific mitochondrial density	D_{mtE}	$D_{mtE} = mtE \cdot m_X^{-1}$	mtEU·kg ⁻¹	4
mitochondrial content, mtE per object X	mtE_X	$mtE_X = mtE \cdot N_X^{-1}$	mtEU·x ⁻¹	5
O₂ flow and flux				
flow, system	I_{O_2}	internal flow	mol·s ⁻¹	6
volume-specific flux	J_{V,O_2}	$J_{V,O_2} = I_{O_2} \cdot V^{-1}$	mol·s ⁻¹ ·m ⁻³	7
flow per object X	I_{X,O_2}	$I_{X,O_2} = J_{V,O_2} \cdot C_{NX}^{-1}$	mol·s ⁻¹ ·x ⁻¹	8
mass-specific flux	J_{mX,O_2}	$J_{mX,O_2} = J_{V,O_2} \cdot C_{mX}^{-1}$	mol·s ⁻¹ ·kg ⁻¹	9
mitochondria-specific flux	J_{mtE,O_2}	$J_{mtE,O_2} = J_{V,O_2} \cdot C_{mtE}^{-1}$	mol·s ⁻¹ ·mtEU ⁻¹	10

- 962 1 The SI prefix k is used for the SI base unit of mass (kg = 1,000 g). In praxis, various SI prefixes are
 963 used for convenience, to make numbers easily readable, e.g., 1 mg tissue, cell or mitochondrial mass
 964 instead of 0.000001 kg.
- 965 2 In case sample $X = \text{cells}$, the object number concentration is $C_{N_{\text{cell}}} = N_{\text{cell}} \cdot V^{-1}$, and volume may be
 966 expressed in [dm³ ≡ L] or [cm³ = mL]. See **Table 5** for different object types.
- 967 3 mt-concentration is an experimental variable, dependent on sample concentration: (1) $C_{mtE} = mtE \cdot V^{-1}$;
 968 (2) $C_{mtE} = mtE_X \cdot C_{NX}$; (3) $C_{mtE} = C_{mX} \cdot D_{mtE}$.
- 969 4 If the amount of mitochondria, mtE , is expressed as mitochondrial mass, then D_{mtE} is the mass
 970 fraction of mitochondria in the sample. If mtE is expressed as mitochondrial volume, V_{mt} , and the
 971 mass of sample, m_X , is replaced by volume of sample, V_X , then D_{mtE} is the volume fraction of
 972 mitochondria in the sample.
- 973 5 $mtE_X = mtE \cdot N_X^{-1} = C_{mtE} \cdot C_{NX}^{-1}$.
- 974 6 O₂ can be replaced by other chemicals B to study different reactions, e.g., ATP, H₂O₂, or
 975 compartmental translocations, e.g., Ca²⁺.
- 976 7 I_{O_2} and V are defined per instrument chamber as a system of constant volume (and constant
 977 temperature), which may be closed or open. I_{O_2} is abbreviated for I_{O_2r} —the metabolic or internal O₂
 978 flow of the chemical reaction r in which O₂ is consumed—hence the negative stoichiometric number,
 979 $\nu_{O_2} = -1$. $I_{O_2r} = d_r n_{O_2} / dt \cdot \nu_{O_2}^{-1}$. If r includes all chemical reactions in which O₂ participates, then $d_r n_{O_2} = dn_{O_2}$
 980 $- d_e n_{O_2}$, where dn_{O_2} is the change in the amount of O₂ in the instrument chamber and $d_e n_{O_2}$ is the
 981 amount of O₂ added externally to the system. At steady state, by definition $dn_{O_2} = 0$, hence $d_r n_{O_2} = -$
 982 $d_e n_{O_2}$.

- 983 8 J_{V,O_2} is an experimental variable, expressed per volume of the instrument chamber.
 984 9 I_{X,O_2} is a physiological variable, depending on the size of entity X .
 985 10 There are many ways to normalize for a mitochondrial marker, that are used in different experimental
 986 approaches: (1) $J_{mtE,O_2} = J_{V,O_2} \cdot C_{mtE}^{-1}$; (2) $J_{mtE,O_2} = J_{V,O_2} \cdot C_{mX}^{-1} \cdot D_{mtE}^{-1} = J_{mX,O_2} \cdot D_{mtE}^{-1}$; (3) $J_{mtE,O_2} =$
 987 $J_{V,O_2} \cdot C_{NX}^{-1} \cdot mtE_X^{-1} = I_{X,O_2} \cdot mtE_X^{-1}$; (4) $J_{mtE,O_2} = I_{O_2} \cdot mtE^{-1}$. The mt-elemental unit [mtEU] varies between
 988 different mt-markers.
 989
 990

Table 5. Sample types, X , abbreviations, and quantification.

Identity of sample	X	N_X	Mass ^a	Volume	mt-Marker
mitochondrial preparation	mtprep	[x]	[kg]	[m ³]	[mtEU]
isolated mitochondria	imt		m_{mt}	V_{mt}	mtE
tissue homogenate	thom		m_{thom}		mtE_{thom}
permeabilized tissue	pti		m_{pti}		mtE_{pti}
permeabilized fibre	pfi		m_{pfi}		mtE_{pfi}
permeabilized cell	pce	N_{pce}	M_{pce}	V_{pce}	mtE_{pce}
intact cell	ce	N_{ce}	M_{ce}	V_{ce}	mtE_{ce}
Organism	org	N_{org}	M_{org}	V_{org}	

^a Instead of mass, frequently the wet weight or dry weight is stated, W_w or W_d .
 m_X is mass of the sample [kg], M_X is mass of the object [kg·x⁻¹].

Number concentration, C_{NX} : C_{NX} is the experimental *number concentration* of sample X . In the case of cells or animals, *e.g.*, nematodes, $C_{NX} = N_X/V$ [x·L⁻¹], where N_X is the number of cells or organisms in the chamber (**Table 4**).

Flow per object, I_{X,O_2} : A special case of normalization is encountered in respiratory studies with permeabilized (or intact) cells. If respiration is expressed per cell, the O₂ flow per measurement system is replaced by the O₂ flow per cell, I_{cell,O_2} (**Table 4**). O₂ flow can be calculated from volume-specific O₂ flux, J_{V,O_2} [nmol·s⁻¹·L⁻¹] (per V of the measurement chamber [L]), divided by the number concentration of cells, $C_{Nce} = N_{ce}/V$ [cell·L⁻¹], where N_{ce} is the number of cells in the chamber. Cellular O₂ flow can be compared between cells of identical size. To take into account changes and differences in cell size, normalization is required to obtain cell size-specific or mitochondrial marker-specific O₂ flux (Renner *et al.* 2003).

The complexity changes when the sample is a whole organism studied as an experimental model. The scaling law in respiratory physiology reveals a strong interaction of O₂ consumption and individual body mass of an organism, since *basal* metabolic rate (flow) does not increase linearly with body mass, whereas *maximum* mass-specific O₂ flux, \dot{V}_{O_2max} or \dot{V}_{O_2peak} , is approximately constant across a large range of individual body mass (Weibel and Hoppeler 2005), with individuals, breeds, and species deviating substantially from this relationship. \dot{V}_{O_2peak} of human endurance athletes is 60 to 80 mL O₂·min⁻¹·kg⁻¹ body mass, converted to J_{M,O_2peak} of 45 to 60 nmol·s⁻¹·g⁻¹ (Gnaiger 2014; **Table 6**).

3.4. Normalization for mitochondrial content

Tissues can contain multiple cell populations that may have distinct mitochondrial subtypes. Mitochondria undergo dynamic fission and fusion cycles, and can exist in multiple stages and sizes which may be altered by a range of factors. The isolation of mitochondria (often achieved through differential centrifugation) can therefore yield a subsample of the mitochondrial types present in a tissue, depending on isolation protocols utilized (*e.g.*, centrifugation speed). This possible bias should be taken into account when planning experiments using isolated mitochondria. Different sizes of mitochondria are enriched at specific centrifugation speeds, which is used for isolation of mitochondrial subpopulations.

1024 Part of the mitochondrial content of a tissue is lost during preparation of isolated
 1025 mitochondria. The fraction of mitochondria in the isolate is expressed as mitochondrial
 1026 recovery. At a high mitochondrial recovery the sample of isolated mitochondria is more
 1027 representative of the total mitochondrial population than in preparations characterized by low
 1028 recovery. Determination of the mitochondrial recovery and yield is based on measurement of
 1029 the concentration of a mitochondrial marker in the tissue homogenate, $C_{mtE,thom}$, which
 1030 simultaneously provides information on the specific mitochondrial density in the sample.

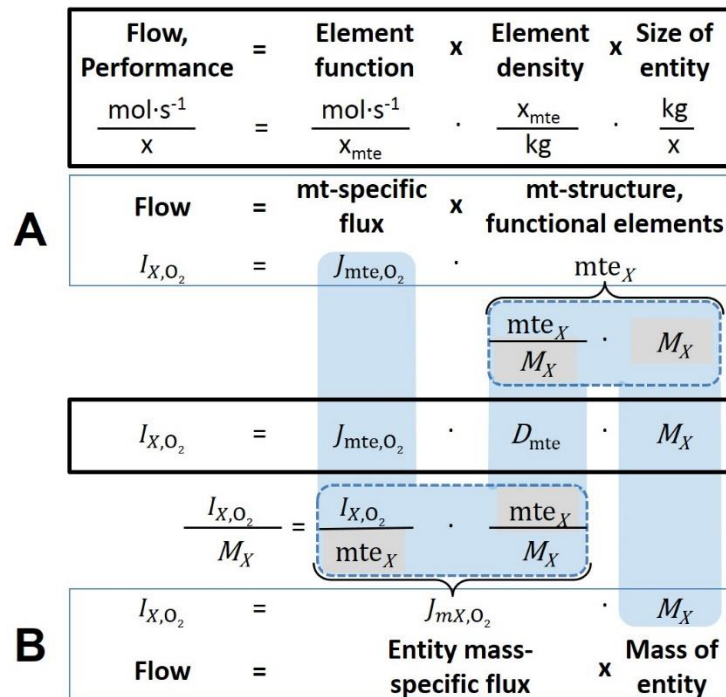
1031 Normalization is a problematic subject; it is essential to consider the question of the study.
 1032 If the study aims at comparing tissue performance—such as the effects of a treatment on a
 1033 specific tissue, then normalization can be successful, using tissue mass or protein content, for
 1034 example. However, if the aim is to find differences on mitochondrial function independent of
 1035 mitochondrial density (**Table 4**), then normalization to a mitochondrial marker is imperative
 1036 (**Fig. 7**). One cannot assume that quantitative changes in various markers—such as
 1037 mitochondrial proteins—necessarily occur in parallel with one another. It should be established
 1038 that the marker chosen is not selectively altered by the performed treatment. In conclusion, the
 1039 normalization must reflect the question under investigation to reach a satisfying answer. On the
 1040 other hand, the goal of comparing results across projects and institutions requires
 1041 standardization on normalization for entry into a databank.

1042 **Mitochondrial concentration, C_{mtE} , and mitochondrial markers:** Mitochondrial
 1043 concentration in the tissue and the measurement chamber are quantified as (1) a physiological
 1044 output that is the result of mitochondrial biogenesis and degradation, and (2) a quantity for
 1045 normalization in functional analyses. Mitochondrial organelles comprise a dynamic cellular
 1046 reticulum in various states of fusion and fission. Hence, the definition of an "amount" of
 1047 mitochondria is often misconceived: mitochondria cannot be counted reliably as a number of
 1048 occurring elements. Therefore, quantification of the "amount" of mitochondria depends on the
 1049 measurement of chosen mitochondrial markers. 'Mitochondria are the structural and functional
 1050 elemental units of cell respiration' (Gnaiger 2014). The quantity of a mitochondrial marker can
 1051 reflect the amount of *mitochondrial elements*, mtE , expressed in various mitochondrial
 1052 elemental units [mtEU] specific for each measured mt-marker (**Table 4**). However, since
 1053 mitochondrial quality may change in response to stimuli—particularly in mitochondrial
 1054 dysfunction and after exercise training (Pesta *et al.* 2011; Campos *et al.* 2017)—some markers
 1055 can vary while others are unchanged: (1) Mitochondrial volume and membrane area are
 1056 structural markers, whereas mitochondrial protein mass is frequently used as a marker for
 1057 isolated mitochondria. (2) Molecular and enzymatic mitochondrial markers (amounts or
 1058 activities) can be selected as matrix markers, *e.g.*, citrate synthase activity, mtDNA; mtIM-
 1059 markers, *e.g.*, cytochrome *c* oxidase activity, aa_3 content, cardiolipin, or mtOM-markers, *e.g.*,
 1060 TOM20. (3) Extending the measurement of mitochondrial marker enzyme activity to
 1061 mitochondrial pathway capacity, ET- or OXPHOS-capacity can be considered as an integrative
 1062 functional mitochondrial marker.

1063 Depending on the type of mitochondrial marker, the mitochondrial elements, mtE , are
 1064 expressed in marker-specific units. It is recommended to distinguish *experimental*
 1065 *mitochondrial concentration*, $C_{mtE} = mtE/V$ and *physiological mitochondrial density*, $D_{mtE} =$
 1066 mtE/m_X . Then mitochondrial density is the amount of mitochondrial elements per mass of tissue,
 1067 which is a biological variable (**Fig. 7**). The experimental variable is mitochondrial density
 1068 multiplied by sample mass concentration in the measuring chamber, $C_{mtE} = D_{mtE} \cdot C_{mX}$, or
 1069 mitochondrial content multiplied by sample number concentration, $C_{mtE} = mtE_X \cdot C_{NX}$ (**Table 4**).

1070 **Mitochondria-specific flux, J_{mtE,O_2} :** Volume-specific metabolic O_2 flux depends on: (1)
 1071 the sample concentration in the volume of the instrument chamber, C_{mX} , or C_{NX} ; (2) the
 1072 mitochondrial density in the sample, $D_{mtE} = mtE/m_X$ or $mtE_X = mtE/N_X$; and (3) the specific
 1073 mitochondrial activity or performance per elemental mitochondrial unit, $J_{mtE,O_2} = J_{V,O_2}/C_{mtE}$

1074 [mol·s⁻¹·mtEU⁻¹] (Table 4). Obviously, the numerical results for J_{mtE,O_2} vary with the type of
 1075 mitochondrial marker chosen for measurement of mtE and $C_{mtE} = mtE/V$ [mtEU·m⁻³].
 1076



1077 **Fig. 7. Structure-function analysis of performance of an organism, organ or tissue, or a**
 1078 **cell (sample entity, X). O₂ flow, I_{X,O_2} , is the product of performance per functional element**
 1079 **(element function, mitochondria-specific flux), element density (mitochondrial density,**
 1080 **D_{mtE}), and size of entity X (mass, M_X). (A) Structured analysis: performance is the product of**
 1081 **mitochondrial function (mt-specific flux) and structure (functional elements; D_{mtE} times mass**
 1082 **of X). (B) Unstructured analysis: performance is the product of entity mass-specific flux, J_{mX,O_2}**
 1083 **$= I_{X,O_2}/M_X = I_{O_2}/m_X$ [mol·s⁻¹·kg⁻¹] and size of entity, expressed as mass of X; $M_X = m_X \cdot N_X^{-1}$**
 1084 **[kg·x⁻¹]. See Table 4 for further explanation of quantities and units. Modified from Gnaiger**
 1085 **(2014).**
 1086

1087 3.5. Evaluation of mitochondrial markers

1089 Different methods are implicated in the quantification of mitochondrial markers and have
 1090 different strengths. Some problems are common for all mitochondrial markers, mtE : (1)
 1091 Accuracy of measurement is crucial, since even a highly accurate and reproducible
 1092 measurement of O₂ flux results in an inaccurate and noisy expression normalized for a biased
 1093 and noisy measurement of a mitochondrial marker. This problem is acute in mitochondrial
 1094 respiration because the denominators used (the mitochondrial markers) are often small moieties
 1095 of which accurate and precise determination is difficult. This problem can be avoided when O₂
 1096 fluxes measured in substrate-uncoupler-inhibitor titration protocols are normalized for flux in
 1097 a defined respiratory reference state, which is used as an *internal* marker and yields flux control
 1098 ratios, *FCRs*. *FCRs* are independent of any *externally* measured markers and, therefore, are
 1099 statistically robust, considering the limitations of ratios in general (Jasienski and Bazzaz 1999).
 1100 *FCRs* indicate qualitative changes of mitochondrial respiratory control, with highest
 1101 quantitative resolution, separating the effect of mitochondrial density or concentration on J_{mX,O_2}
 1102 and I_{X,O_2} from that of function per elemental mitochondrial marker, J_{mtE,O_2} (Pesta *et al.* 2011;
 1103 Gnaiger 2014). (2) If mitochondrial quality does not change and only the amount of
 1104 mitochondria varies as a determinant of mass-specific flux, any marker is equally qualified in
 1105 principle; then in practice selection of the optimum marker depends only on the accuracy and
 1106

1107 precision of measurement of the mitochondrial marker. (3) If mitochondrial flux control ratios
1108 change, then there may not be any best mitochondrial marker. In general, measurement of
1109 multiple mitochondrial markers enables a comparison and evaluation of normalization for a
1110 variety of mitochondrial markers. Particularly during postnatal development, the activity of
1111 marker enzymes—such as cytochrome *c* oxidase and citrate synthase—follows different time
1112 courses (Drahota *et al.* 2004). Evaluation of mitochondrial markers in healthy controls is
1113 insufficient for providing guidelines for application in the diagnosis of pathological states and
1114 specific treatments.

1115 In line with the concept of the respiratory control ratio (Chance and Williams 1955a), the
1116 most readily used normalization is that of flux control ratios and flux control factors (Gnaiger
1117 2014). Selection of the state of maximum flux in a protocol as the reference state has the
1118 advantages of: (1) internal normalization; (2) statistical linearization of the response in the range
1119 of 0 to 1; and (3) consideration of maximum flux for integrating a large number of elemental
1120 steps in the OXPHOS- or ET-pathways. This reduces the risk of selecting a functional marker
1121 that is specifically altered by the treatment or pathology, yet increases the chance that the highly
1122 integrative pathway is disproportionately affected, *e.g.*, the OXPHOS- rather than ET-pathway
1123 in case of an enzymatic defect in the phosphorylation-pathway. In this case, additional
1124 information can be obtained by reporting flux control ratios based on a reference state which
1125 indicates stable tissue-mass specific flux. Stereological determination of mitochondrial content
1126 via two-dimensional transmission electron microscopy can have limitations due to the dynamics
1127 of mitochondrial size (Meinild Lundby *et al.* 2017). Accurate determination of three-
1128 dimensional volume by two-dimensional microscopy can be both time consuming and
1129 statistically challenging (Larsen *et al.* 2012).

1130 The validity of using mitochondrial marker enzymes (citrate synthase activity, Complex
1131 I–IV amount or activity) for normalization of flux is limited in part by the same factors that
1132 apply to flux control ratios. Strong correlations between various mitochondrial markers and
1133 citrate synthase activity (Reichmann *et al.* 1985; Boushel *et al.* 2007; Mogensen *et al.* 2007)
1134 are expected in a specific tissue of healthy subjects and in disease states not specifically
1135 targeting citrate synthase. Citrate synthase activity is acutely modifiable by exercise
1136 (Tonkonogi *et al.* 1997; Leek *et al.* 2001). Evaluation of mitochondrial markers related to a
1137 selected age and sex cohort cannot be extrapolated to provide recommendations for
1138 normalization in respirometric diagnosis of disease, in different states of development and
1139 ageing, different cell types, tissues, and species. mtDNA normalized to nDNA via qPCR is
1140 correlated to functional mitochondrial markers including OXPHOS- and ET-capacity in some
1141 cases (Puntschart *et al.* 1995; Wang *et al.* 1999; Menshikova *et al.* 2006; Boushel *et al.* 2007),
1142 but lack of such correlations have been reported (Menshikova *et al.* 2005; Schultz and Wiesner
1143 2000; Pesta *et al.* 2011). Several studies indicate a strong correlation between cardiolipin
1144 content and increase in mitochondrial function with exercise (Menshikova *et al.* 2005;
1145 Menshikova *et al.* 2007; Larsen *et al.* 2012; Faber *et al.* 2014), but its use as a general
1146 mitochondrial biomarker in disease remains questionable.

1147

1148 3.6. Conversion: units

1149

1150 Many different units have been used to report the rate of oxygen consumption, OCR
1151 (**Table 6**). *SI* base units provide the common reference to introduce the theoretical principles
1152 (**Fig. 6**), and are used with appropriately chosen *SI* prefixes to express numerical data in the
1153 most practical format, with an effort towards unification within specific areas of application
1154 (**Table 7**). Reporting data in *SI* units—including the mole [mol], coulomb [C], joule [J], and
1155 second [s]—should be encouraged, particularly by journals which propose the use of *SI* units.

1156

1157
1158
1159
1160**Table 6. Conversion of various units used in respirometry and ergometry.** e^- is the number of electrons or reducing equivalents. z_B is the charge number of entity B.

1 Unit	x	Multiplication factor	SI-unit	Note
ng.atom O \cdot s $^{-1}$	(2 e $^-$)	0.5	nmol O $_2$ \cdot s $^{-1}$	
ng.atom O \cdot min $^{-1}$	(2 e $^-$)	8.33	pmol O $_2$ \cdot s $^{-1}$	
natom O \cdot min $^{-1}$	(2 e $^-$)	8.33	pmol O $_2$ \cdot s $^{-1}$	
nmol O $_2$ \cdot min $^{-1}$	(4 e $^-$)	16.67	pmol O $_2$ \cdot s $^{-1}$	
nmol O $_2$ \cdot h $^{-1}$	(4 e $^-$)	0.2778	pmol O $_2$ \cdot s $^{-1}$	
mL O $_2$ \cdot min $^{-1}$ at STPD ^a		0.744	μ mol O $_2$ \cdot s $^{-1}$	1
W = J/s at -470 kJ/mol O $_2$		-2.128	μ mol O $_2$ \cdot s $^{-1}$	
mA = mC \cdot s $^{-1}$	($z_{H^+} = 1$)	10.36	nmol H $^+$ \cdot s $^{-1}$	2
mA = mC \cdot s $^{-1}$	($z_{O_2} = 4$)	2.59	nmol O $_2$ \cdot s $^{-1}$	2
nmol H $^+$ \cdot s $^{-1}$	($z_{H^+} = 1$)	0.09649	mA	3
nmol O $_2$ \cdot s $^{-1}$	($z_{O_2} = 4$)	0.38594	mA	3

1161
1162
1163
1164
1165
1166
1167
1168
1169
1170

- 1 At standard temperature and pressure dry (STPD: 0 °C = 273.15 K and 1 atm = 101.325 kPa = 760 mmHg), the molar volume of an ideal gas, V_m , and V_{m,O_2} is 22.414 and 22.392 L \cdot mol $^{-1}$, respectively. Rounded to three decimal places, both values yield the conversion factor of 0.744. For comparison at **NTPD** (20 °C), V_{m,O_2} is 24.038 L \cdot mol $^{-1}$. Note that the SI standard pressure is 100 kPa.
- 2 The multiplication factor is $10^6/(z_B \cdot F)$.
- 3 The multiplication factor is $z_B \cdot F/10^6$.

Table 7. Conversion of units with preservation of numerical values.

Name	Frequently used unit	Equivalent unit	Note
volume-specific flux, J_{V,O_2}	pmol \cdot s $^{-1}$ \cdot mL $^{-1}$	nmol \cdot s $^{-1}$ \cdot L $^{-1}$	1
	nmol \cdot s $^{-1}$ \cdot L $^{-1}$	mol \cdot s $^{-1}$ \cdot m $^{-3}$	
cell-specific flow, I_{O_2}	pmol \cdot s $^{-1}$ \cdot 10 $^{-6}$ cells	amol \cdot s $^{-1}$ \cdot cell $^{-1}$	2
	pmol \cdot s $^{-1}$ \cdot 10 $^{-9}$ cells	zmol \cdot s $^{-1}$ \cdot cell $^{-1}$	3
cell number concentration, C_{Nce}	10 6 cells \cdot mL $^{-1}$	10 9 cells \cdot L $^{-1}$	
mitochondrial protein concentration, C_{mtE}	0.1 mg \cdot mL $^{-1}$	0.1 g \cdot L $^{-1}$	
mass-specific flux, J_{m,O_2}	pmol \cdot s $^{-1}$ \cdot mg $^{-1}$	nmol \cdot s $^{-1}$ \cdot g $^{-1}$	4
catabolic power, P_k	μ W \cdot 10 $^{-6}$ cells	pW \cdot cell $^{-1}$	1
V olume	1,000 L	m 3 (1,000 kg)	
	L	dm 3 (kg)	
	mL	cm 3 (g)	
	μ L	mm 3 (mg)	
	fL	μ m 3 (pg)	5
amount of substance concentration	M = mol \cdot L $^{-1}$	mol \cdot dm $^{-3}$	

1171
1172
1173
1174
1175

- 1 pmol: picomole = 10 $^{-12}$ mol
- 2 amol: attomole = 10 $^{-18}$ mol
- 3 zmol: zeptomole = 10 $^{-21}$ mol
- 4 nmol: nanomole = 10 $^{-9}$ mol
- 5 fL: femtolitre = 10 $^{-15}$ L

1176 Although volume is expressed as m^3 using the *SI* base unit, the litre [dm^3] is a
 1177 conventional unit of volume for concentration and is used for most solution chemical kinetics.
 1178 If one multiplies $I_{\text{cell},\text{O}_2}$ by $C_{N_{\text{cell}}}$, then the result will not only be the amount of O_2 [mol]
 1179 consumed per time [s^{-1}] in one litre [L^{-1}], but also the change in the concentration of oxygen per
 1180 second (for any volume of an ideally closed system). This is ideal for kinetic modeling as it
 1181 blends with chemical rate equations where concentrations are typically expressed in $\text{mol}\cdot\text{L}^{-1}$
 1182 (Wagner *et al.* 2011). In studies of multinuclear cells—such as differentiated skeletal muscle
 1183 cells—it is easy to determine the number of nuclei but not the total number of cells. A
 1184 generalized concept, therefore, is obtained by substituting cells by nuclei as the sample entity.
 1185 This does not hold, however, for enucleated platelets.

1186 For studies of cells, we recommend that respiration be expressed, as far as possible, as:
 1187 (1) O_2 flux normalized for a mitochondrial marker, for separation of the effects of mitochondrial
 1188 quality and content on cell respiration (this includes *FCRs* as a normalization for a functional
 1189 mitochondrial marker); (2) O_2 flux in units of cell volume or mass, for comparison of respiration
 1190 of cells with different cell size (Renner *et al.* 2003) and with studies on tissue preparations, and
 1191 (3) O_2 flow in units of attomole (10^{-18} mol) of O_2 consumed in a second by each cell
 1192 [$\text{amol}\cdot\text{s}^{-1}\cdot\text{cell}^{-1}$], numerically equivalent to [$\text{pmol}\cdot\text{s}^{-1}\cdot 10^{-6}$ cells]. This convention allows
 1193 information to be easily used when designing experiments in which oxygen consumption must
 1194 be considered. For example, to estimate the volume-specific O_2 flux in an instrument chamber
 1195 that would be expected at a particular cell number concentration, one simply needs to multiply
 1196 the flow per cell by the number of cells per volume of interest. This provides the amount of O_2
 1197 [mol] consumed per time [s^{-1}] per unit volume [L^{-1}]. At an O_2 flow of $100 \text{ amol}\cdot\text{s}^{-1}\cdot\text{cell}^{-1}$ and a
 1198 cell density of $10^9 \text{ cells}\cdot\text{L}^{-1}$ ($10^6 \text{ cells}\cdot\text{mL}^{-1}$), the volume-specific O_2 flux is $100 \text{ nmol}\cdot\text{s}^{-1}\cdot\text{L}^{-1}$ (100
 1199 $\text{pmol}\cdot\text{s}^{-1}\cdot\text{mL}^{-1}$).

1200 ET-capacity in human cell types including HEK 293, primary HUVEC and fibroblasts
 1201 ranges from 50 to $180 \text{ amol}\cdot\text{s}^{-1}\cdot\text{cell}^{-1}$, measured in intact cells in the noncoupled state (see
 1202 Gnaiger 2014). At $100 \text{ amol}\cdot\text{s}^{-1}\cdot\text{cell}^{-1}$ corrected for *Rox*, the current across the mt-membranes,
 1203 $I_{e\text{H}^+}$, approximates $193 \text{ pA}\cdot\text{cell}^{-1}$ or 0.2 nA per cell. See Rich (2003) for an extension of
 1204 quantitative bioenergetics from the molecular to the human scale, with a transmembrane proton
 1205 flux equivalent to 520 A in an adult at a catabolic power of -110 W. Modelling approaches
 1206 illustrate the link between protonmotive force and currents (Willis *et al.* 2016).

1207 We consider isolated mitochondria as powerhouses and proton pumps as molecular
 1208 machines to relate experimental results to energy metabolism of the intact cell. The cellular
 1209 $\text{P}\gg/\text{O}_2$ based on oxidation of glycogen is increased by the glycolytic (fermentative) substrate-
 1210 level phosphorylation of 3 $\text{P}\gg/\text{Glyc}$ or 0.5 mol $\text{P}\gg$ for each mol O_2 consumed in the complete
 1211 oxidation of a mol glycosyl unit (Glyc). Adding 0.5 to the mitochondrial $\text{P}\gg/\text{O}_2$ ratio of 5.4
 1212 yields a bioenergetic cell physiological $\text{P}\gg/\text{O}_2$ ratio close to 6. Two NADH equivalents are
 1213 formed during glycolysis and transported from the cytosol into the mitochondrial matrix, either
 1214 by the malate-aspartate shuttle or by the glycerophosphate shuttle resulting in different
 1215 theoretical yields of ATP generated by mitochondria, the energetic cost of which potentially
 1216 must be taken into account. Considering also substrate-level phosphorylation in the TCA cycle,
 1217 this high $\text{P}\gg/\text{O}_2$ ratio not only reflects proton translocation and OXPHOS studied in isolation,
 1218 but integrates mitochondrial physiology with energy transformation in the living cell (Gnaiger
 1219 1993a).

1220
1221

1222 4. Conclusions

1223
1224
1225
1226

MitoEAGLE can serve as a gateway to better diagnose mitochondrial respiratory defects
 linked to genetic variation, age-related health risks, sex-specific mitochondrial performance,
 lifestyle with its effects on degenerative diseases, and thermal and chemical environment. The

1227 present recommendations on coupling control states and rates, linked to the concept of the
 1228 protonmotive force, are focused on studies with mitochondrial preparations. These will be
 1229 extended in a series of reports on pathway control of mitochondrial respiration, respiratory
 1230 states in intact cells, and harmonization of experimental procedures.

1231

1232 **Table 8. Terms, symbols, and units.**
 1233
 1234

1235 Term	Symbol	SI unit	Links and comments
1237			
1238 alternative quinol oxidase	AOX		Fig. 1
1239 amount of substance B	n_B	[mol]	
1240 Complexes I to IV	CI to CIV		respiratory ET Complexes; Fig. 1
1241 concentration of substance B	$c_B = n_B \cdot V^{-1}$; [B]	[mol·m ⁻³]	Box 2
1242 electron transfer system	ETS		
1243 flow, for substance B	I_B	[mol·s ⁻¹]	system-related extensive quantity; Fig. 6
1244 flux, for substance B	J_B	<i>varies</i>	size-specific quantity; Fig. 6
1245 inorganic phosphate	P_i		
1246 LEAK	LEAK		Tab. 1
1247 mass of sample X	m_X	[kg]	Tab. 4
1248 mass of entity X	M_X	[kg]	Tab. 4
1249 MITOCARTA			https://www.broadinstitute.org/scientific-community/science/programs/metabolic-disease-program/publications/mitocarta/mitocarta-in-0
1250			
1251			
1252			
1253			
1254 MitoPedia			http://www.bioblast.at/index.php/MitoPedia
1255 mitochondria or mitochondrial	mt		Box 1
1256 mitochondrial DNA	mtDNA		Box 1
1257 mitochondrial concentration	$C_{mtE} = mtE \cdot V^{-1}$	[mtEU·m ⁻³]	Tab. 4
1258 mitochondrial content	$mtE_X = mtE \cdot N_X^{-1}$	[mtEU·x ⁻¹]	Tab. 4
1259 mitochondrial elemental unit	mtEU	<i>varies</i>	Tab. 4, specific units for mt-marker
1260 mitochondrial inner membrane	mtIM		MIM is widely used, and M is replaced by mt as abbreviation for mitochondria;
1261			Box 1
1262			
1263 mitochondrial outer membrane	mtOM		MOM is widely used, and M is replaced by mt as abbreviation for mitochondria;
1264			Box 1
1265			
1266 mitochondrial recovery	Y_{mtE}		
1267 mitochondrial yield	$Y_{mtE/m}$		$Y_{mtE/m} = Y_{mtE} \cdot D_{mtE}$
1268 negative	neg		Fig. 2
1269 number concentration of X	C_{NX}	[x·m ⁻³]	Tab. 4
1270 number of entities X	N_X	[x]	Tab. 4, Fig. 7
1271 number of entity B	N_B	[x]	Tab. 4
1272 oxidative phosphorylation	OXPPOS		Tab. 1
1273 oxygen concentration	$c_{O_2} = n_{O_2} \cdot V^{-1}$; [O ₂]	[mol·m ⁻³]	Section 3.2
1274 phosphorylation of ADP to ATP	P»		Section 2.2
1275 positive	pos		Fig. 2
1276 proton in the negative compartment	H ⁺ _{neg}		Fig. 2
1277 proton in the positive compartment	H ⁺ _{pos}		Fig. 2
1278 rate of electron transfer in ET state	E		ET-capacity; Tab. 1
1279 rate of LEAK respiration	L		Tab. 1
1280 rate of oxidative phosphorylation	P		OXPPOS capacity; Tab. 1
1281 rate of residual oxygen consumption	R_{ox}		Tab. 1
1282 residual oxygen consumption	ROX		Tab. 1
1283 specific mitochondrial density	$D_{mtE} = mtE \cdot m_X^{-1}$	[mtEU·kg ⁻¹]	Tab. 7
1284 volume	V	[m ³]	
1285 weight, dry weight	W_d	[kg]	used as mass of sample X; Fig. 6
1286 weight, wet weight	W_w	[kg]	used as mass of sample X; Fig. 6
1287			

1288 The optimal choice for expressing mitochondrial and cell respiration (**Box 3**) as O₂ flow
1289 per biological system, and normalization for specific tissue-markers (volume, mass, protein)
1290 and mitochondrial markers (volume, protein, content, mtDNA, activity of marker enzymes,
1291 respiratory reference state) is guided by the scientific question under study. Interpretation of
1292 the obtained data depends critically on appropriate normalization, and therefore reporting rates
1293 merely as nmol·s⁻¹ is discouraged, since it restricts the analysis to intra-experimental
1294 comparison of relative (qualitative) differences. Expressing O₂ consumption per cell may not
1295 be possible when dealing with tissues. For studies with mitochondrial preparations, we
1296 recommend that normalizations be provided as far as possible: (1) on a per cell basis as O₂ flow
1297 (a biophysical normalization); (2) per g cell or tissue protein, or per cell or tissue mass as mass-
1298 specific O₂ flux (a cellular normalization); and (3) per mitochondrial marker as mt-specific flux
1299 (a mitochondrial normalization). With information on cell size and the use of multiple
1300 normalizations, maximum potential information is available (Renner *et al.* 2003; Wagner *et al.*
1301 2011; Gnaiger 2014).

1302 When using isolated mitochondria, total mitochondrial protein is a frequently applied
1303 mitochondrial marker, the use of which is restricted to isolated mitochondria. The
1304 mitochondrial recovery and yield, and experimental criteria for evaluation of purity versus
1305 integrity should be reported. Mitochondrial markers—such as citrate synthase activity as an
1306 enzymatic matrix marker—provide a link to the tissue of origin on the basis of calculating the
1307 mitochondrial recovery, *i.e.*, the fraction of mitochondrial marker obtained from a unit mass of
1308 tissue.

1309

1310 **Box 3: Mitochondrial and cell respiration**

1311

1312 Mitochondrial and cell respiration is the process of exergonic and exothermic energy
1313 transformation in which scalar redox reactions are coupled to vectorial ion translocation across
1314 a semipermeable membrane, which separates the small volume of a bacterial cell or
1315 mitochondrion from the larger volume of its surroundings. The electrochemical exergy can be
1316 partially conserved in the phosphorylation of ADP to ATP or in ion pumping, or dissipated in
1317 an electrochemical short-circuit. Respiration is thus clearly distinguished from fermentation as
1318 the counterpart of cellular core energy metabolism. Respiration is separated in mitochondrial
1319 preparations from the partial contribution of fermentative pathways of the intact cell. Residual
1320 oxygen consumption—as measured after inhibition of mitochondrial electron transfer—does
1321 not belong to the class of catabolic reactions and is, therefore, subtracted from total oxygen
1322 consumption to obtain baseline-corrected respiration.

1323

1324 Terms and symbols are summarized in **Table 8**. Their use will facilitate transdisciplinary
1325 communication and support further developments towards a consistent theory of bioenergetics
1326 and mitochondrial physiology. Technical terms related to and defined with normal words can
1327 be used as index terms in databases, support the creation of ontologies towards semantic
1328 information processing (MitoPedia), and help in communicating analytical findings as
1329 impactful data-driven stories. ‘*Making data available without making it understandable may be
1330 worse than not making it available at all*’ (National Academies of Sciences, Engineering, and
1331 Medicine 2018). This is a call to carefully contribute to FAIR principles (Findable, Accessible,
1332 Interoperable, Reusable) for the sharing of scientific data.

1333

1334 **Acknowledgements**

1335 We thank M. Beno for management assistance. Supported by COST Action CA15203
1336 MitoEAGLE and K-Regio project MitoFit (E.G.).

1337

1338 **Competing financial interests:** E.G. is founder and CEO of Oroboros Instruments, Innsbruck,
1339 Austria.

1340

1341 5. References

1342

1343 Altmann R (1894) Die Elementarorganismen und ihre Beziehungen zu den Zellen. Zweite vermehrte Auflage.
1344 Verlag Von Veit & Comp, Leipzig:160 pp.

1345 Beard DA (2005) A biophysical model of the mitochondrial respiratory system and oxidative phosphorylation.
1346 PLoS Comput Biol 1(4):e36.

1347 Benda C (1898) Weitere Mitteilungen über die Mitochondria. Verh Dtsch Physiol Ges:376-83.

1348 Birkedal R, Laasmaa M, Vendelin M (2014) The location of energetic compartments affects energetic
1349 communication in cardiomyocytes. Front Physiol 5:376.

1350 Breton S, Beaupré HD, Stewart DT, Hoeh WR, Blier PU (2007) The unusual system of doubly uniparental
1351 inheritance of mtDNA: isn't one enough? Trends Genet 23:465-74.

1352 Brown GC (1992) Control of respiration and ATP synthesis in mammalian mitochondria and cells. Biochem J
1353 284:1-13.

1354 Calvo SE, Klauser CR, Mootha VK (2016) MitoCarta2.0: an updated inventory of mammalian mitochondrial
1355 proteins. Nucleic Acids Research 44:D1251-7.

1356 Calvo SE, Julien O, Clauser KR, Shen H, Kamer KJ, Wells JA, Mootha VK (2017) Comparative analysis of
1357 mitochondrial N-termini from mouse, human, and yeast. Mol Cell Proteomics 16:512-23.

1358 Campos JC, Queliconi BB, Bozi LHM, Bechara LRG, Dourado PMM, Andres AM, Jannig PR, Gomes KMS,
1359 Zambelli VO, Rocha-Resende C, Guatimosim S, Brum PC, Mochly-Rosen D, Gottlieb RA, Kowaltowski AJ,
1360 Ferreira JCB (2017) Exercise reestablishes autophagic flux and mitochondrial quality control in heart failure.
1361 Autophagy 13:1304-317.

1362 Canton M, Luvisetto S, Schmehl I, Azzone GF (1995) The nature of mitochondrial respiration and
1363 discrimination between membrane and pump properties. Biochem J 310:477-81.

1364 Chance B, Williams GR (1955a) Respiratory enzymes in oxidative phosphorylation. I. Kinetics of oxygen
1365 utilization. J Biol Chem 217:383-93.

1366 Chance B, Williams GR (1955b) Respiratory enzymes in oxidative phosphorylation: III. The steady state. J Biol
1367 Chem 217:409-27.

1368 Chance B, Williams GR (1955c) Respiratory enzymes in oxidative phosphorylation. IV. The respiratory chain. J
1369 Biol Chem 217:429-38.

1370 Chance B, Williams GR (1956) The respiratory chain and oxidative phosphorylation. Adv Enzymol Relat Subj
1371 Biochem 17:65-134.

1372 Cobb LJ, Lee C, Xiao J, Yen K, Wong RG, Nakamura HK, Mehta HH, Gao Q, Ashur C, Huffman DM, Wan J,
1373 Muzumdar R, Barzilai N, Cohen P (2016) Naturally occurring mitochondrial-derived peptides are age-
1374 dependent regulators of apoptosis, insulin sensitivity, and inflammatory markers. Aging (Albany NY) 8:796-
1375 809.

1376 Cohen ER, Cvitas T, Frey JG, Holmström B, Kuchitsu K, Marquardt R, Mills I, Pavese F, Quack M, Stohner J,
1377 Strauss HL, Takami M, Thor HL (2008) Quantities, units and symbols in physical chemistry, IUPAC Green
1378 Book, 3rd Edition, 2nd Printing, IUPAC & RSC Publishing, Cambridge.

1379 Cooper H, Hedges LV, Valentine JC, eds (2009) The handbook of research synthesis and meta-analysis. Russell
1380 Sage Foundation.

1381 Coopersmith J (2010) Energy, the subtle concept. The discovery of Feynman's blocks from Leibnitz to Einstein.
1382 Oxford University Press:400 pp.

1383 Cummins J (1998) Mitochondrial DNA in mammalian reproduction. Rev Reprod 3:172-82.

1384 Dai Q, Shah AA, Garde RV, Yonish BA, Zhang L, Medvitz NA, Miller SE, Hansen EL, Dunn CN, Price TM
1385 (2013) A truncated progesterone receptor (PR-M) localizes to the mitochondrion and controls cellular
1386 respiration. Mol Endocrinol 27:741-53.

1387 Divakaruni AS, Brand MD (2011) The regulation and physiology of mitochondrial proton leak. Physiology
1388 (Bethesda) 26:192-205.

1389 Doerrier C, Garcia-Souza LF, Krumschnabel G, Wohlfarter Y, Mészáros AT, Gnaiger E (2018) High-Resolution
1390 Fluorescence Respirometry and OXPHOS protocols for human cells, permeabilized fibres from small biopsies of
1391 muscle and isolated mitochondria. Methods Mol. Biol. (in press)

1392 Doskey CM, van't Erve TJ, Wagner BA, Buettner GR (2015) Moles of a substance per cell is a highly
1393 informative dosing metric in cell culture. PLOS ONE 10:e0132572.

1394 Drahotová Z, Milerová M, Stieglerová A, Houstek J, Ostádal B (2004) Developmental changes of cytochrome c
1395 oxidase and citrate synthase in rat heart homogenate. Physiol Res 53:119-22.

1396 Duarte FV, Palmeira CM, Rolo AP (2014) The role of microRNAs in mitochondria: small players acting wide.
1397 Genes (Basel) 5:865-86.

1398 Ernster L, Schatz G (1981) Mitochondria: a historical review. J Cell Biol 91:227s-55s.

- 1399 Estabrook RW (1967) Mitochondrial respiratory control and the polarographic measurement of ADP:O ratios.
1400 *Methods Enzymol* 10:41-7.
- 1401 Faber C, Zhu ZJ, Castellino S, Wagner DS, Brown RH, Peterson RA, Gates L, Barton J, Bickett M, Hagerty L,
1402 Kimbrough C, Sola M, Bailey D, Jordan H, Elangbam CS (2014) Cardiolipin profiles as a potential
1403 biomarker of mitochondrial health in diet-induced obese mice subjected to exercise, diet-restriction and
1404 ephedrine treatment. *J Appl Toxicol* 34:1122-9.
- 1405 Fell D (1997) Understanding the control of metabolism. Portland Press.
- 1406 Garlid KD, Beavis AD, Ratkje SK (1989) On the nature of ion leaks in energy-transducing membranes. *Biochim*
1407 *Biophys Acta* 976:109-20.
- 1408 Garlid KD, Semrad C, Zinchenko V. Does redox slip contribute significantly to mitochondrial respiration? In:
1409 Schuster S, Rigoulet M, Ouhabi R, Mazat J-P, eds (1993) *Modern trends in biothermokinetics*. Plenum Press,
1410 New York, London:287-93.
- 1411 Gerö D, Szabo C (2016) Glucocorticoids suppress mitochondrial oxidant production via upregulation of
1412 uncoupling protein 2 in hyperglycemic endothelial cells. *PLoS One* 11:e0154813.
- 1413 Gnaiger E. Efficiency and power strategies under hypoxia. Is low efficiency at high glycolytic ATP production a
1414 paradox? In: *Surviving Hypoxia: Mechanisms of Control and Adaptation*. Hochachka PW, Lutz PL, Sick T,
1415 Rosenthal M, Van den Thillart G, eds (1993a) CRC Press, Boca Raton, Ann Arbor, London, Tokyo:77-109.
- 1416 Gnaiger E (1993b) Nonequilibrium thermodynamics of energy transformations. *Pure Appl Chem* 65:1983-2002.
- 1417 Gnaiger E (2001) Bioenergetics at low oxygen: dependence of respiration and phosphorylation on oxygen and
1418 adenosine diphosphate supply. *Respir Physiol* 128:277-97.
- 1419 Gnaiger E (2009) Capacity of oxidative phosphorylation in human skeletal muscle. New perspectives of
1420 mitochondrial physiology. *Int J Biochem Cell Biol* 41:1837-45.
- 1421 Gnaiger E (2014) Mitochondrial pathways and respiratory control. An introduction to OXPHOS analysis. 4th ed.
1422 *Mitochondr Physiol Network* 19.12. Oroboros MiPNet Publications, Innsbruck:80 pp.
- 1423 Gnaiger E, Méndez G, Hand SC (2000) High phosphorylation efficiency and depression of uncoupled respiration
1424 in mitochondria under hypoxia. *Proc Natl Acad Sci USA* 97:11080-5.
- 1425 Greggio C, Jha P, Kulkarni SS, Lagarrigue S, Broskey NT, Boutant M, Wang X, Conde Alonso S, Ofori E,
1426 Auwerx J, Cantó C, Amati F (2017) Enhanced respiratory chain supercomplex formation in response to
1427 exercise in human skeletal muscle. *Cell Metab* 25:301-11.
- 1428 Hinkle PC (2005) P/O ratios of mitochondrial oxidative phosphorylation. *Biochim Biophys Acta* 1706:1-11.
- 1429 Hofstadter DR (1979) Gödel, Escher, Bach: An eternal golden braid. A metaphorical fugue on minds and
1430 machines in the spirit of Lewis Carroll. Harvester Press:499 pp.
- 1431 Illaste A, Laasmaa M, Peterson P, Vendelin M (2012) Analysis of molecular movement reveals latticelike
1432 obstructions to diffusion in heart muscle cells. *Biophys J* 102:739-48.
- 1433 Jasienski M, Bazzaz FA (1999) The fallacy of ratios and the testability of models in biology. *Oikos* 84:321-26.
- 1434 Jephthina N, Beraud N, Sepp M, Birkedal R, Vendelin M (2011) Permeabilized rat cardiomyocyte response
1435 demonstrates intracellular origin of diffusion obstacles. *Biophys J* 101:2112-21.
- 1436 Klepinin A, Ounpuu L, Guzun R, Chekulayev V, Timohhina N, Tepp K, Shevchuk I, Schlattner U, Kaambre T
1437 (2016) Simple oxygraphic analysis for the presence of adenylate kinase 1 and 2 in normal and tumor cells. *J*
1438 *Bioenerg Biomembr* 48:531-48.
- 1439 Klingenberg M (2017) UCP1 - A sophisticated energy valve. *Biochimie* 134:19-27.
- 1440 Koit A, Shevchuk I, Ounpuu L, Klepinin A, Chekulayev V, Timohhina N, Tepp K, Puurand M, Truu L, Heck K,
1441 Valvere V, Guzun R, Kaambre T (2017) Mitochondrial respiration in human colorectal and breast cancer
1442 clinical material is regulated differently. *Oxid Med Cell Longev* 1372640.
- 1443 Komlódi T, Tretter L (2017) Methylene blue stimulates substrate-level phosphorylation catalysed by succinyl-
1444 CoA ligase in the citric acid cycle. *Neuropharmacology* 123:287-98.
- 1445 Lane N (2005) Power, sex, suicide: mitochondria and the meaning of life. Oxford University Press:354 pp.
- 1446 Larsen S, Nielsen J, Neigaard Nielsen C, Nielsen LB, Wibrand F, Stride N, Schroder HD, Boushel RC, Helge
1447 JW, Dela F, Hey-Mogensen M (2012) Biomarkers of mitochondrial content in skeletal muscle of healthy
1448 young human subjects. *J Physiol* 590:3349-60.
- 1449 Lee C, Zeng J, Drew BG, Sallam T, Martin-Montalvo A, Wan J, Kim SJ, Mehta H, Hevener AL, de Cabo R,
1450 Cohen P (2015) The mitochondrial-derived peptide MOTS-c promotes metabolic homeostasis and reduces
1451 obesity and insulin resistance. *Cell Metab* 21:443-54.
- 1452 Lee SR, Kim HK, Song IS, Youm J, Dizon LA, Jeong SH, Ko TH, Heo HJ, Ko KS, Rhee BD, Kim N, Han J
1453 (2013) Glucocorticoids and their receptors: insights into specific roles in mitochondria. *Prog Biophys Mol*
1454 *Biol* 112:44-54.
- 1455 Leek BT, Mudaliar SR, Henry R, Mathieu-Costello O, Richardson RS (2001) Effect of acute exercise on citrate
1456 synthase activity in untrained and trained human skeletal muscle. *Am J Physiol Regul Integr Comp Physiol*
1457 *280*:R441-7.
- 1458 Lemieux H, Blier PU, Gnaiger E (2017) Remodeling pathway control of mitochondrial respiratory capacity by
1459 temperature in mouse heart: electron flow through the Q-junction in permeabilized fibers. *Sci Rep* 7:2840.

- 1460 Lenaz G, Tioli G, Falasca AI, Genova ML (2017) Respiratory supercomplexes in mitochondria. In: Mechanisms
1461 of primary energy trasduction in biology. M Wikstrom (ed) Royal Society of Chemistry Publishing, London,
1462 UK:296-337.
- 1463 Margulis L (1970) Origin of eukaryotic cells. New Haven: Yale University Press.
- 1464 Meinild Lundby AK, Jacobs RA, Gehrig S, de Leur J, Hauser M, Bonne TC, Flück D, Dandanell S, Kirk N,
1465 Kaech A, Ziegler U, Larsen S, Lundby C (2018) Exercise training increases skeletal muscle mitochondrial
1466 volume density by enlargement of existing mitochondria and not de novo biogenesis. *Acta Physiol* 222,
1467 e12905.
- 1468 Menshikova EV, Ritov VB, Fairfull L, Ferrell RE, Kelley DE, Goodpaster BH (2006) Effects of exercise on
1469 mitochondrial content and function in aging human skeletal muscle. *J Gerontol A Biol Sci Med Sci* 61:534-
1470 40.
- 1471 Menshikova EV, Ritov VB, Ferrell RE, Azuma K, Goodpaster BH, Kelley DE (2007) Characteristics of skeletal
1472 muscle mitochondrial biogenesis induced by moderate-intensity exercise and weight loss in obesity. *J Appl*
1473 *Physiol* (1985) 103:21-7.
- 1474 Menshikova EV, Ritov VB, Toledo FG, Ferrell RE, Goodpaster BH, Kelley DE (2005) Effects of weight loss
1475 and physical activity on skeletal muscle mitochondrial function in obesity. *Am J Physiol Endocrinol Metab*
1476 288:E818-25.
- 1477 Miller GA (1991) The science of words. Scientific American Library New York:276 pp.
- 1478 Mitchell P (1961) Coupling of phosphorylation to electron and hydrogen transfer by a chemi-osmotic type of
1479 mechanism. *Nature* 191:144-8.
- 1480 Mitchell P (2011) Chemiosmotic coupling in oxidative and photosynthetic phosphorylation. *Biochim Biophys*
1481 *Acta Bioenergetics* 1807:1507-38.
- 1482 Mogensen M, Sahlin K, Fernström M, Glintborg D, Vind BF, Beck-Nielsen H, Højlund K (2007) Mitochondrial
1483 respiration is decreased in skeletal muscle of patients with type 2 diabetes. *Diabetes* 56:1592-9.
- 1484 Mohr PJ, Phillips WD (2015) Dimensionless units in the SI. *Metrologia* 52:40-7.
- 1485 Moreno M, Giacco A, Di Munno C, Goglia F (2017) Direct and rapid effects of 3,5-diiodo-L-thyronine (T2).
1486 *Mol Cell Endocrinol* 7207:30092-8.
- 1487 Morrow RM, Picard M, Derbeneva O, Leipzig J, McManus MJ, Gousspillou G, Barbat-Artigas S, Dos Santos C,
1488 Hepple RT, Murdock DG, Wallace DC (2017) Mitochondrial energy deficiency leads to hyperproliferation of
1489 skeletal muscle mitochondria and enhanced insulin sensitivity. *Proc Natl Acad Sci U S A* 114:2705-10.
- 1490 Murley A, Nunnari J (2016) The emerging network of mitochondria-organelle contacts. *Mol Cell* 61:648-53.
- 1491 National Academies of Sciences, Engineering, and Medicine (2018) International coordination for science data
1492 infrastructure: Proceedings of a workshop—in brief. Washington, DC: The National Academies Press. doi:
1493 <https://doi.org/10.17226/25015>.
- 1494 Paradies G, Paradies V, De Benedictis V, Ruggiero FM, Petrosillo G (2014) Functional role of cardiolipin in
1495 mitochondrial bioenergetics. *Biochim Biophys Acta* 1837:408-17.
- 1496 Pesta D, Gnaiger E (2012) High-Resolution Respirometry. OXPHOS protocols for human cells and
1497 permeabilized fibres from small biopsies of human muscle. *Methods Mol Biol* 810:25-58.
- 1498 Pesta D, Hoppel F, Macek C, Messner H, Faulhaber M, Kobel C, Parson W, Burtscher M, Schocke M, Gnaiger
1499 E (2011) Similar qualitative and quantitative changes of mitochondrial respiration following strength and
1500 endurance training in normoxia and hypoxia in sedentary humans. *Am J Physiol Regul Integr Comp Physiol*
1501 301:R1078–87.
- 1502 Price TM, Dai Q (2015) The role of a mitochondrial progesterone receptor (PR-M) in progesterone action.
1503 *Semin Reprod Med* 33:185-94.
- 1504 Puchowicz MA, Varnes ME, Cohen BH, Friedman NR, Kerr DS, Hoppel CL (2004) Oxidative phosphorylation
1505 analysis: assessing the integrated functional activity of human skeletal muscle mitochondria – case studies.
1506 *Mitochondrion* 4:377-85. Puntschart A, Claassen H, Jostarndt K, Hoppeler H, Billeter R (1995) mRNAs of
1507 enzymes involved in energy metabolism and mtDNA are increased in endurance-trained athletes. *Am J*
1508 *Physiol* 269:C619-25.
- 1509 Quiros PM, Mottis A, Auwerx J (2016) Mitonuclear communication in homeostasis and stress. *Nat Rev Mol*
1510 *Cell Biol* 17:213-26.
- 1511 Reichmann H, Hoppeler H, Mathieu-Costello O, von Bergen F, Pette D (1985) Biochemical and ultrastructural
1512 changes of skeletal muscle mitochondria after chronic electrical stimulation in rabbits. *Pflugers Arch* 404:1-
1513 9.
- 1514 Renner K, Amberger A, Konwalinka G, Gnaiger E (2003) Changes of mitochondrial respiration, mitochondrial
1515 content and cell size after induction of apoptosis in leukemia cells. *Biochim Biophys Acta* 1642:115-23.
- 1516 Rich P (2003) Chemiosmotic coupling: The cost of living. *Nature* 421:583.
- 1517 Rostovtseva TK, Sheldon KL, Hassanzadeh E, Monge C, Saks V, Bezrukov SM, Sackett DL (2008) Tubulin
1518 binding blocks mitochondrial voltage-dependent anion channel and regulates respiration. *Proc Natl Acad Sci*
1519 *USA* 105:18746-51.

- 1520 Rustin P, Parfait B, Chretien D, Bourgeron T, Djouadi F, Bastin J, Rötig A, Munnich A (1996) Fluxes of
1521 nicotinamide adenine dinucleotides through mitochondrial membranes in human cultured cells. *J Biol Chem*
1522 271:14785-90.
- 1523 Saks VA, Veksler VI, Kuznetsov AV, Kay L, Sikk P, Tiivel T, Tranqui L, Olivares J, Winkler K, Wiedemann F,
1524 Kunz WS (1998) Permeabilised cell and skinned fiber techniques in studies of mitochondrial function in
1525 vivo. *Mol Cell Biochem* 184:81-100.
- 1526 Salabei JK, Gibb AA, Hill BG (2014) Comprehensive measurement of respiratory activity in permeabilized cells
1527 using extracellular flux analysis. *Nat Protoc* 9:421-38.
- 1528 Sazanov LA (2015) A giant molecular proton pump: structure and mechanism of respiratory complex I. *Nat Rev*
1529 *Mol Cell Biol* 16:375-88.
- 1530 Schneider TD (2006) Claude Shannon: biologist. The founder of information theory used biology to formulate
1531 the channel capacity. *IEEE Eng Med Biol Mag* 25:30-3.
- 1532 Schönfeld P, Dymkowska D, Wojtczak L (2009) Acyl-CoA-induced generation of reactive oxygen species in
1533 mitochondrial preparations is due to the presence of peroxisomes. *Free Radic Biol Med* 47:503-9.
- 1534 Schultz J, Wiesner RJ (2000) Proliferation of mitochondria in chronically stimulated rabbit skeletal muscle--
1535 transcription of mitochondrial genes and copy number of mitochondrial DNA. *J Bioenerg Biomembr* 32:627-
1536 34.
- 1537 Simson P, Jepihhina N, Laasmaa M, Peterson P, Birkedal R, Vendelin M (2016) Restricted ADP movement in
1538 cardiomyocytes: Cytosolic diffusion obstacles are complemented with a small number of open mitochondrial
1539 voltage-dependent anion channels. *J Mol Cell Cardiol* 97:197-203.
- 1540 Stucki JW, Ineichen EA (1974) Energy dissipation by calcium recycling and the efficiency of calcium transport
1541 in rat-liver mitochondria. *Eur J Biochem* 48:365-75.
- 1542 Tonkonogi M, Harris B, Sahlin K (1997) Increased activity of citrate synthase in human skeletal muscle after a
1543 single bout of prolonged exercise. *Acta Physiol Scand* 161:435-6.
- 1544 Waczulikova I, Habodaszova D, Cagalinec M, Ferko M, Ulicna O, Mateasik A, Sikurova L, Ziegelhöffer A
1545 (2007) Mitochondrial membrane fluidity, potential, and calcium transients in the myocardium from acute
1546 diabetic rats. *Can J Physiol Pharmacol* 85:372-81.
- 1547 Wagner BA, Venkataraman S, Buettner GR (2011) The rate of oxygen utilization by cells. *Free Radic Biol Med*
1548 51:700-712.
- 1549 Wang H, Hiatt WR, Barstow TJ, Brass EP (1999) Relationships between muscle mitochondrial DNA content,
1550 mitochondrial enzyme activity and oxidative capacity in man: alterations with disease. *Eur J Appl Physiol*
1551 *Occup Physiol* 80:22-7.
- 1552 Watt IN, Montgomery MG, Runswick MJ, Leslie AG, Walker JE (2010) Bioenergetic cost of making an
1553 adenosine triphosphate molecule in animal mitochondria. *Proc Natl Acad Sci U S A* 107:16823-7.
- 1554 Weibel ER, Hoppeler H (2005) Exercise-induced maximal metabolic rate scales with muscle aerobic capacity. *J*
1555 *Exp Biol* 208:1635-44.
- 1556 White DJ, Wolff JN, Pierson M, Gemmell NJ (2008) Revealing the hidden complexities of mtDNA inheritance.
1557 *Mol Ecol* 17:4925-42.
- 1558 Wikström M, Hummer G (2012) Stoichiometry of proton translocation by respiratory complex I and its
1559 mechanistic implications. *Proc Natl Acad Sci U S A* 109:4431-6.
- 1560 Willis WT, Jackman MR, Messer JI, Kuzmiak-Glancy S, Glancy B (2016) A simple hydraulic analog model of
1561 oxidative phosphorylation. *Med Sci Sports Exerc* 48:990-1000.